Development of nanoparticle-polymer based composite films and its effect on bacterial biofilm formation

Saranya. P

Department of Biotechnology and Medical Engineering
National Institute of Technology Rourkela

Development of nanoparticle-polymer based composite films and its effect on bacterial biofilm formation

Thesis submitted in partial fulfillment

of the requirements of the degree of

Master of Technology

in

Biotechnology and Medical Engineering
(*Specialization*: *Biotechnology*)

by

Saranya. P

(Roll Number: 215BM2005)

based on research carried out

under the supervision of

Prof. Subhankar Paul

May, 2017

Department of Biotechnology and Medical Engineering
National Institute of Technology Rourkela

Department of Biotechnology and Medical Engineering
National Institute of Technology Rourkela

Prof. Subhankar Paul
Associate Professor

May 30, 2017

Supervisor's Certificate

This is to certify that the work presented in the research project entitled "*Development of nanoparticle-polymer based composite films and its effect on bacterial biofilm formation*"submitted by *Saranya. P*, Roll Number 215BM2005, is a record of original research carried out by her under my supervision and guidance in partial fulfillment of the requirements of the degree of *Master of Technology* in *Biotechnology*. Neither this thesis nor any part of it has been submitted earlier for any degree or diploma to any institute or university in India or abroad.

_____
Subhankar Paul

Declaration of Originality

I, *Saranya. P*, Roll Number *215BM2005* hereby declare that this dissertation entitled *Development of nanoparticle-polymer based composite films and its effect on bacterial biofilm formation* presents my original work carried out as a postgraduate student of NIT Rourkela and, to the best of my knowledge, contains no material previously published or written by another person, nor any material presented by me for the award of any degree or diploma of NIT Rourkela or any other institution. Any contribution made to this research by others, with whom I have worked at NIT Rourkela or elsewhere, is explicitly acknowledged in the dissertation. Works of other authors cited in this dissertation have been duly acknowledged under the sections "Reference" or "Bibliography". I have also submitted my original research records to the scrutiny committee for evaluation of my dissertation.

I am fully aware that in case of any non-compliance detected in future, the Senate of NIT Rourkela may withdraw the degree awarded to me on the basis of the present dissertation.

May 30, 2017
NIT Rourkela

Saranya. P

Acknowledgment

This work was carried out at the Department of Biotechnology and Medical Engineering, National Institute of Technology, Rourkela, Orissa, under the supervision of **Prof. Subhankar Paul**.

I am deeply grateful to my supervisor, Prof. S Paul whose insights and encouragements have helped me in shaping up this thesis. I would also like to thank him for the useful scientific discussions and critical review of the entire thesis work from time to time. Last one years were a fantastic amalgamation of scientific deliberations, discussions, doubts, agreements and disagreements which has helped me in developing my thoughts regarding various issues pertaining to research and life in general, especially planning research and its execution.

I would like to express my sincere thanks to the PhD scholar. Prathap.S for his suggestions and encouragement to perform my project work.

I would thank my parents and friends for being supportive throughput the entire course of the thesis. I thank the almighty, merciful and passionate for providing me the opportunity to step in the world of science.

May 30, 2017 *Saranya. P*

NIT Rourkela Roll Number: 215BM2005

ABSTRACT

Antimicrobial surfaces and materials are being emerging to control infectious microorganisms and are important in our day to day life and effectually protect the public health from pollutants including organic, inorganic and biological substances in wide range forms. Developing hybrid nanocomposites coatings that exhibit multiple approach of preventing biofilm formation provides a new generation material to combat against sessile bacterial community. In this study, we fabricated a hybrid nanoparticles (silver nanoparticles-AgNPs, Graphene oxide-GO) and polymer base (chitosan-Ch) which shows both the antibacterial and anti-adhesion properties to prevent and kill the bacteria. The fabrication and characterization of the various composite films GO-Ch, GO-AgNPs, Ch-AgNPs and GO-Ch-AgNPs were analyzed by UV–visible spectroscopy, Transmission Electron Microscopy (TEM), X-ray diffraction (XRD), Field Emission Scanning Electron Microscopy (FESEM) and Fourier transform Infra red spectroscopy (FTIR). The antibiofilm activity is evaluated against two model bacteria relative to composite. The silver impregnated nanocomposites exhibit higher antibacterial activity by capture killing process and GO-Ch film exhibit anti biofilm activity by anti-adhesion activity. The results obtained in this research provided a potential next generation composite coating against prevention of biofilms.

Keywords*: *Biofilm*; *graphene oxide*; *silver nanoparticle*; *nano composites*; *anti-adhesion*; *anti-biofilm

Contents

List of Figures

List of Abbreviation

$AgNO_3$	Silver nitrate
AgNPs	Silver nanoparticles
B.subtilis	*Bacillus subtilis*
CA	Contact angle
Ch	Chitosan
DNA	Deoxyribonucleic acid
E.coli	*Escherichia coli*
EPS	Extracellular Polymeric Substances
FCC	Face Centered Cubic
FESEM	Field Emission Transmission Electron Microscopy
FT-IR	Fourier Transform Infrared Spectroscopy
GOns	Graphene oxide nanosheets
h	Hour
H_2O_2	Hydrogen peroxide
H_2SO_4	Sulfuric acid
$KMnO_4$	Potassium permanganate
min	Minutes
mL	Milliliter
mm	Millimetre
MPa	Mega Pascal
$NaNO_3$	Sodium nitrate
OD	Optical Density
PBS	Phosphate Buffered Saline
pH	Potential of hydrogen
SAED	Selected Area Diffraction Pattern
SPR	Surface Plasmon Resonance
TEM	Transmission Electron Microscopy
UTM	Universal Testing Machine
XRD	X-Ray Diffraction
ZOI	Zone of Inhibition

Chapter 1

Introduction

1.1 Biofilm formation

Microbial contamination and colonization have always been a problem for human society [1]. Many microorganisms can attach to surfaces and form biofilms which are protected by a matrix named extracellular polymeric substances (EPS) [2]. Biofilms can be found in hospital, industrial and domestic settings. Indeed, life of microbes inside a biofilm represents the predominant way of growth of microorganism. The extracellular matrix provides structure and protection to the community of microbes inside the biofilm [3]. Matured biofilms have a few noticeable characteristics include formation of macro colonies of more than thousands of micro cells which is fenced by channels filled with fluid. Biofilm forming bacteria naturally impart resistance to a wide range of antibiotic and many other antimicrobial agents.

1.2 Anti-microbial coatings

The removal of biofilms is usually accomplished by acid/alkaline based chemical detergents and mechanical force. But their efficiency largely depends upon temperature, pH, concentration and time of exposure of the chemicals [2, 4]. Antimicrobial surfaces and materials are being emerging to control infectious microorganisms and are important in our day to day life and effectually protect the public health from pollutants including organic, inorganic and biological substances in wide range forms [5, 6]. Recent improvements in the field of nanotechnology and material science are the driving force to develop multi approach antimicrobial coatings [7]. A number of metal and its oxide nanoparticles based on iron, zinc, silver, copper, gold, magnesium, selenium, zinc [8–10] and non-metallic nanoparticles such as nitric oxide, chitosan and calcium hydroxide showed antibiofilm activity against sessile community bacteria [1, 11, 12].

1.3 Graphene oxide nanosheets

Graphene oxide (GO) is a chemically modified two dimensional graphene material, made of dense honeycomb structure of the monolayers of carbon atoms containing hydroxyl, carbonyl, carboxyl and epoxy groups [13–15]. In modern research, immense consideration has been centered on graphene and its nanomaterials due to their incredible capacity in various applications such as energy storage, electrochemical devices, catalysis, enzyme adsorption, drug delivery, cell imaging, and biosensors. Specifically, graphene oxide, chemically exfoliated from graphite oxide is found to be a futuristic material for biological and electrical applications due to its excellent aqueous amphiphilicity, surface functionalization ability, fluorescence quenching ability processability, and surface-enhanced Raman scattering properties.

Graphene oxide is easily dispersible with in aqueous media and also possesses excellent antimicrobial properties. Additionally, GO is non-cytotoxic at low concentrations, in spite of the fact that it has some adverse effects at high concentrations. GO kills bacteria by physical damage upon direct contact with bacterial cell membranes with its sharp sheet edges [16]. Moreover, GO has large surface area and extra ordinary dispersive nature in water with high stability [17]. Therefore, GO can be used as the platform for preparing stable nanocomposites to prevent aggregation of metal nanoparticles. Individual graphene or GO and graphene-based composites have pulled in such a great amount of consideration from researchers everywhere throughout the world that their applications have been extended to microbial eradication. Recently, many research works demonstrated the synergistic antibacterial effect of GO-AgNP nanohybrid [18, 19].

1.4 Chitosan polymer

The advancement of biomaterials is playing a critical aspect in the areas of health and hygiene. The preparation of nanocomposites is the best route to improve the properties of biopolymeric materials and also to accomplish the possibility of imparting new desirable properties. Chitosan is a standout amongst the most common polymer for biopolymeric advanced materials. It is an amazing natural polymer with broad range of applications in wide variety of fields such as biomedical, food, textiles, and the paper industry . Chitosan serves as the only natural polymer that can be formed as solution, thin films, fibers or hydrogel and it is made up of β-1, 4 linked glucosamine and N-acetyl glucosamine distributed randomly and it is easily processed by deacetylation of chitin. Chitosan has been noticed to be biodegradable, non-toxic, and biocompatible, with antimicrobial characteristic.

The main reason for the antimicrobial activity of chitosan is the protonation of the amino group of the chitosan chain in acid solution, causing chitosan to be positively charged and interact with negatively charged cell membranes of the microbes, result in the leakage of

protein and other intracellular constituents of the microbes [20]. Chitosan was thus utilized as a polymeric matrix films that exhibit potential antimicrobial properties against various groups of microorganisms.

1.5 Silver nanoparticles

Among the variety of investigated metal nanoparticles, silver nanoparticles (AgNPs) have an extraordinary antibacterial action [12, 21, 22] and silver has long been perceived for its powerful antimicrobial applications and can be utilized all alone or as nanocomposites for enhanced stability. The three possible factors for the bactericidal activity of AgNPs include contact killing of cellular membrane by AgNP itself, the release of silver (Ag) ions and the reactive oxygen species generation (ROS) [23–26]. The tendency of AgNPs to aggregate in colloidal state lessens its antibacterial effect [27]. Also, size of the silver nanoparticles plays a crucial part in the antibacterial property [28–30]. The promising strategy to overcome the colloidal instability issue is to immobilize the AgNPs over the surface matrix [31]. But the residues of silver ions in treated water and nanosilver had been proclaimed to cause detrimental effects to health. In addition, silver nanoparticles are somewhat expensive. Therefore, there are always attempts to explore materials with equal or better bactericidal properties that are eco-friendly and cost-effective.

1.6 Nanocomposites

The model polymer chitosan contains abundant hydroxyl and amino group which strongly binds with the oxygen groups of GO nanosheets results in the enhancement of physical and mechanical strength of the composite film [32]. Graphene oxide can be easily dispersed in water at an individual sheet level, so it is conceivable to prepare graphene oxide and chitosan composite matrix if water is used as the common solvent.

In recent years, the antibacterial potency of metal and carbon-based engineered nanoparticles has been extensively studied. It is considered that equal distribution of AgNp over the surface is very important to achieve the antimicrobial activity. But the aggregation of silver nanoparticles occurs due to the poor colloidal stability reduces its usage as antibacterial material. In order to overcome the aggregation problem, silver nanoparticles should be loaded on the matrix which does not allow aggregation. Graphene oxide nanosheets act as a matrix for the assembly of silver nanoparticles. To further enhance the stability of the composite, biocompatible polymer chitosan (Ch) can be incorporated into GO which coats the AgNPs and the polymer itself has a strong antibacterial effect [33, 34]. In this study, we demonstrated a drop-casting method to prepare AgNP loaded graphene oxide based chitosan films. This method includes the casting a mixture of solution onto a flat petri dish and allowing water to evaporate for film formation [35, 36].

Chapter 2

Literature Review

2.1 Action of GO against bacteria

GO paper acts as an excellent antibacterial material. The interaction of graphene oxide nanosheets with the cell wall of the bacteria result in the disruption of cell membrane [16]. Also, the fabrication of GO thin films is a low cost process because of the cheap availability of this carbon nanomaterial makes it as a eco friendly antibacterial coating. GO enhances the growth of mammalian cell and its shows low cytotoxic effect. The low cytotoxicity of Graphene oxide provoked research groups to assess the antimicrobial effects of GO based materials [37]. A material which shows low mammalian cell cytotoxicity and high antibacterial characteristics has become a novel material in biological applications. A recent finding has reported that Escherichia coli and Staphylococcus aureus showed 50 and 60% reduction in the growth of bacteria due to the contact of GO.

GO sheet size plays a vital role in its antimicrobial efficacy. The lateral dimension of the Graphene oxide sheets is an important factor for the interaction with bacterial surface. Depending upon the particle size of GO it promotes cell adhesion and its distortion of cell wall [38]. Furthermore, the aggregation of GOs also depends upon the lateral dimension of GO sheets. It was confirmed that the strongest antimicrobial efficacy was exhibited by the uniformly dispersed GO sheets .In contrast, aggregated GO sheets enhanced the growth of bacterial cells when grown in LB medium. Highly purified Graphene oxide neither kills nor inhibits bacteria over a wide range of concentration tested over *E.coli* or *S.aureus*. One research suggested that bactericidal effect of GO might be due to the pH and the contamination occurred during GO preparation [39]. However there are no reported results of GO interaction with biofilm bacteria. But anyways interactions of GO with biofilms could be either bactericidal or bacteriostatic.

2.2 Action of Chitosan against bacteria

The pure Chitosan film shows antimicrobial effect with increasing concentration. However, the antimicrobial efficacy of chitosan relies on various factors such as molecular weight, pH,

temperature of the solution and the deacetylation degree of the chitosan [33]. Chitosan gel showed effective inhibition against Staphylococcus aureus compared to Escherichia coli. A proposed model of bactericidal activity described that the electrostatic interaction between chitosan and the cell membrane has two inferences. One is to promote changes in the permeability of the cell wall membrane thereby increasing the internal osmotic pressure to lyse the cell wall. On the other hand, chitosan may interact with the peptidoglycan layer of the bacterial cell wall which will result in the leaking of intracellular proteins and electrolytes [20].

2.3 Action of Silver nanoparticles against bacteria

Among the range of nanoparticles, silver nanoparticles (AgNPs) are the outstanding antibacterial material. It possesses large surface area to interact with the bacteria and also has the unique slow releasing property in to the solution. Even though the anti bacterial mechanism of AgNp is not clearly understood, three possible ways of action of silver nanoparticles against bacteria are proposed. Firstly, slow release of Ag ions, which interrupt the DNA replication. Secondly, direct damage to cell wall membrane. Lastly, ROS (reactive oxygen species) generation [24, 25].

2.4 Synergistic effect of GO-Ch composite

Chitosan and graphene oxide nano composite possess great stability and mechanical stability. The acetic acid was used as the common solvent which provided matrix to blend chitosan with graphene oxide [36]. Also, water can be used as the solvent to mix chitosan with graphene oxide since GO readily disperses in water and can acts as a matrix for chitosan. It is due to the bonding between epoxy group in GO and amide group in chitosan which resulted in the strong interaction between them in order to form high tensile composite.

Also, another possibility is that chitosan forms H-bonding with hydroxyl groups in Graphene oxide. GO nanosheets can induce toxicity towards Gram-negative and Gram-positive bacteria through ROS generation. They predicted that predict that the defects/oxygen vacancy present at the GO surface which can act as sorption center of water molecules will perturb/react with water molecules thus resulting in the formation of the hydroxyl radicals [40]. Hence the antibacterial activity of the GO nanosheets relies on the production of hydroxyl radicals which will attack the carbonyl groups present in the peptide linkages of the cell wall membrane of bacteria thus resulting in the destruction of the bacteria. Chitosan increase the stability of the GO and showed synergistic effect in killing bacteria.

2.5 Synergistic effect of GO-AgNP composite

Graphene oxide and silver nanoparticles exhibit synergistic effect towards *E.coli*. The composite was formed by the adsorption of silver nanoparticle over the surface of Graphene oxide. The two main advantages of this method is to disperse silver nanoparticles well in the GO aqueous matrix and to imbue synergistic action of GO and silver NPs to kill bacteria [18, 36].As already stated, antimicrobial efficacy of GO is size dependent. Larger GOns show better antimicrobial activity than smaller sheets. Also, GO with high number of functional groups can interact in a better way with the bacteria resulted in deposition of cells over GO sheets [18, 41]. GO decorated with silver nanoparticles showed clear halo zone of inhibition whereas GO alone doesn't show growth inhibition zone [19]. The GO- silver NPs composite acted as an anti- adhesion surface to prevent bacterial growth. The composite exhibited more positive charge helps in the interaction of bacteria towards the surface and end up in killing of the bacteria. Most of the researches reported that small and unaggregated silver nanoparticles possess better antimicrobial activity than bigger particles. GO provides better base matrix for the easy dispersion of AgNPs over the surface to act synergistically against bacteria.

2.6 Synergistic effect of Ch-AgNP composite

In recent times, silver nanoparticles dispersed over chitosan matrix act synergistically against bacterial growth [42]. The outer cell wall membrane of Gram negative bacteria mainly consists of lipopolysaccharide made up of phosphate and pyrophosphate groups results in the negative charge of the cell wall. Since chitosan is a cationic polymer, it can easily interact with the cell wall because of its negative charge by simple electrostatic interaction. At pH less than 6.5 chitosan can act over the bacterial cell wall by weak interactions resulted in the destabilization of cell membrane and altered cell permeability. The permeable cell wall makes the entry of AgNPs easy and allows it to act with the thiol group of proteins in the cell wall results in the leakage of intracellular proteins and distortion of cell wall [21]. Also, chitosan can acts as a stabilizer by making amide bond with AgNPs to prevent agglomeration of silver nanoparticles. The adsorption property of chitosan maximizes the bacterial interaction to the surface and helps in capture killing process.

Taking into account the properties of the three fore discussed materials ,the overall objective of the present work focused on the simple, cost effective and environmentally safe preparation of composites (GO-Ch-AgNPs) to evaluate its antibiofilm efficacy against the two model bacteria Gram-negative (*Escherichia coli*) and Gram- positive (*Bacillus subtilis*).

Chapter 3

Materials and Methods

3.1 Materials

Graphite powder, Chitosan flakes, Sodium nitrate, Silver nitrate ($AgNO_3$), Sodium hydroxide (NaOH), Starch, Potassium permanganate ($KMnO_4$), 30% Hydrogen peroxide (H_2O_2), Concentrated Sulphuric acid (H_2SO_4), Hydrochloric acid (HCl), Congo red dye, Coomassie brilliant blue R-250 stain, Nutrient agar, Luria broth, Glucose, Crystal violet dye, Ethanol and Glutaraldehyde were purchased from Hi-media, India. The chemicals used in all experiments are of the pure and analytical grade. All glass wares (test tubes, beakers, measuring cylinder, microscopic glass slides, cover slips and petridishes) were purchased from borosil, India. Centrifuge tubes and micropipette tips used in this project were purchased from Tarsons, India.

3.2 Instrumentation

The UV-visible absorption spectra were recorded with a Perkin-Elmer UV-VIS spectrophotometer Lambda35 in the range of 200-800 nm. The size and morphological aspects of GO and AgNPs were analyzed using Bruker made nano Transmission Electron Microscope (TEM). X-ray diffraction (XRD) patterns were analyzed by Rigaku made X-ray diffractometer with monochromatic CuKα, radiation (λ = 1.5406 Aº) in the scan range of 5° to 80° at a scan rate of 5º min^{-1}. Fourier transform infrared (FTIR) spectra were recorded using Alpha-FTIR (Bruker) spectrometer in the range of wavenumber 4000-400 cm^{-1}. The degree of hydrophobicity of the films was calculated using Kruss CA apparatus for static water contact angle (CA) measurement. The tensile properties of the casted films (dimension = 20 mm ×10 mm ×0.03 mm) were measured with the help of Super Duper Multi National Conglomerates ultimate tensile testing machine (UTM) at temperature of 18º C. The morphology of the composite films and bacterial attachment over composite films were analyzed using Bruker made Nova nanosem Field Emission Scanning Electron Microscopy (FESEM).

3.3 Preparation of base components

3.3.1 Preparation of Graphene oxide nano sheets

Graphene oxide (GO) nano sheets were prepared by modified Hummer's method through oxidation and exfoliation of GO. Briefly, one gram of graphite powder and 0.5 g of sodium nitrate ($NaNO_3$) were dissolved gradually in 23 ml of concentrated Sulfuric acid under magnetic stirrer at 500 rpm for about one hour. Then 3 g of potassium permanganate ($KMnO_4$) was added very slowly to the mixture, while maintaining the temperature below 20ºC. The mixture was allowed to stir for about 2-3 h for complete oxidation. Then 46 ml of distilled water was added slowly and allowed to stir for 30 min since the reaction is highly exothermic and emit toxic gases. After that it was diluted with 140 ml of distilled water followed by the addition of 10 ml 30% (v/v) H_2O_2 solution to stop the reaction until color changes to yellowish brown and no bubbles appear. The sample was washed with 1:10 (v/v) ratio Hydrochloric acid and Millipore water in order to remove metal ions in the mixture. The supernatant was sonicated for 2 h at regular intervals at 0.5 cycle and 80% amplitude for exfoliation of graphene layers to monolayer GO.

3.3.2 Preparation of 1% chitosan solution

Dissolve 1% of chitosan (Ch) in 0.1 M acetic acid under magnetic stirrer at temperature 95ºC for more than one hour till gets dissolved completely. The viscous solution obtained can be used for the composite preparation.

3.3.3 Preparation of silver nanoparticles (AgNPs)

The preparation of starch capped silver nanoparticles is a straight forward process. Briefly, 0.5 mL of 40 mM $AgNO_3$ solution was added slowly to the 14 mL of 1% aqueous soluble starch solution heated in the microwave oven. The whole process should be maintained under uniform temperature of 70ºC. After complete mixing of the components, 6 mL of 20 mM NaOH was added drop wise and further stirred for 15-20 min till the solution color turns to dark brown which illustrates the formation of silver nanoparticles.

3.4 Preparation of colloidal composite solutions and films

The prepared solutions were mixed under magnetic stirring to form uniform colloids and they were further ultrasonicated for equal dispersion. We prepared GO-Ch (1:1), GO-AgNPs (0.01% doped in GO), Ch-AgNPs (0.01% doped in Ch) and GO-Ch-AgNP (0.01% doped in GO-Ch) stable colloidal composites. We carried out a drop-casting method to prepare thin films. This approach includes casting the mixture of colloidal composites onto a petri dish

and allowing it to dry at 40ºC in order to evaporate water for thin film formation. The dried solutions were peeled off as composite films.

3.5 Checking anti-biofilm activity of nanocomposites

3.5.1 Cultivation of Bacterial Strains

The anti biofilm activity of the nanocomposite films were investigated against the biofilm forming Gram negative *Escherichia coli* and Gram positive *Bacillus subtilis*. The strains were cultured in Luria Bertani (LB) broth and grown statically overnight at 37ºC until it reached the OD_{600} of 1.0.

3.5.2 Anti bacterial analysis by Zone of Inhibition test

The agar base of 15 g/L mixed with LB medium was autoclaved firstly. After cooled down to 50ºC, the agar solution was poured into petri dish and allowed to solidify at room temperature. The solidified agar surface was spreaded with 50 µL of bacterial samples (*E.coli* and *B.subtilis*) with Fimbriae OD_{600} of 1.0. The individual and composite films were placed over the spreaded culture and incubated at 37ºC for 24 h to test the zone formation.

3.5.3 Fimbriae production analysis using Congo red agar plate assay

To assess the morphology of fimbriae in *E.coli* and *B.subtilis*, 1 µL overnight culture (OD_{600} = 1) of the bacteria was spotted on the centre of the Congo red agar plate (15 g/L LB agar, 20 µg/ml congo red, 10 µg/ml coomassie brilliant blue mixed in 20 g/L LB medium). In order to measure the effectiveness of the composite films over fimbriae production, films were placed onto the centre of the plate and 1 µL culture was placed over the films and fimbriae production was assessed after 24-48 h of incubation at 37ºC.

3.5.4 Swarming motility assay

To assay the swarming motility of the bacteria, 1µL overnight culture (OD_{600} = 1) of the bacteria was spotted on the centre of the LB agar (0.5%) supplemented with glucose (0.8%). In order to measure the effectiveness of the composite films over swarming motility of the bacteria , films were placed onto the centre of the plate and 1 µL culture was placed over the films and swarming pattern was observed after 24-48 h of incubation at 37ºC.

3.5.5 In vitro biofilm static assay

To evaluate the amount of biofilm formed by the bacteria with the presence of individual and composite films, we used an in vitro biofilm static assay using crystal violet dye. Briefly,

all the films were cut into 2 ×1 cm and placed individually in the test tubes for autoclaving. The OD_{600} of 1.0 bacterial culture were diluted to 1:100 and 5 mL of diluted culture was added alone as a control variant and to each autoclaved test tubes with the films and kept for incubation at 37ºC for 48 h. After incubation, the culture and the films were dumped out and test tubes were washed with the sterile Millipore water in order to remove the unattached cells from the walls of test tube. Followed by washing, 6.25 mL of 0.1% crystal violet dye to each test tube and allowed to incubate for 15 min. Then, rinse the test tubes for 3 times to remove excess stain and allowed the test tubes to dry for an hour. Finally, add 6.25 mL of 80% ethanol to each test tube and allowed to stand for 15 min till the dye dissolve completely in the ethanol. The absorbance of crystal violet in ethanol solution was taken in UV-visible spectrophotometer at OD_{595} which is directly proportional to the amount of biofilm formed by the bacteria.

3.5.6 Bacterial attachment over incubated films

The attachment and biofilm formation of *E.coli* and *B.subtilis* over the surface of the films were observed by Field Emission Scanning Electron Microscopy. The films incubated inside the bacterial culture were washed with Phosphate Buffered Saline (PBS) and cells over films were fixed using glutaraldehyde followed by dehydration using different concentrations of ethanol and dried overnight to visualize bacteria.

Chapter 4

Results and Discussion

4.1 Preparation of base and nanocomposite solution

The photographic images of colloidal suspension of the base components and the composites are shown in Figure 4.1. The brown color of GO solution shows the successful oxidation of graphite to graphene oxide [14]. The yellow color AgNP solution showed the formation of unaggregated nanoparticles and it is further confirmed by UV-Visible spectra and TEM analysis[43].

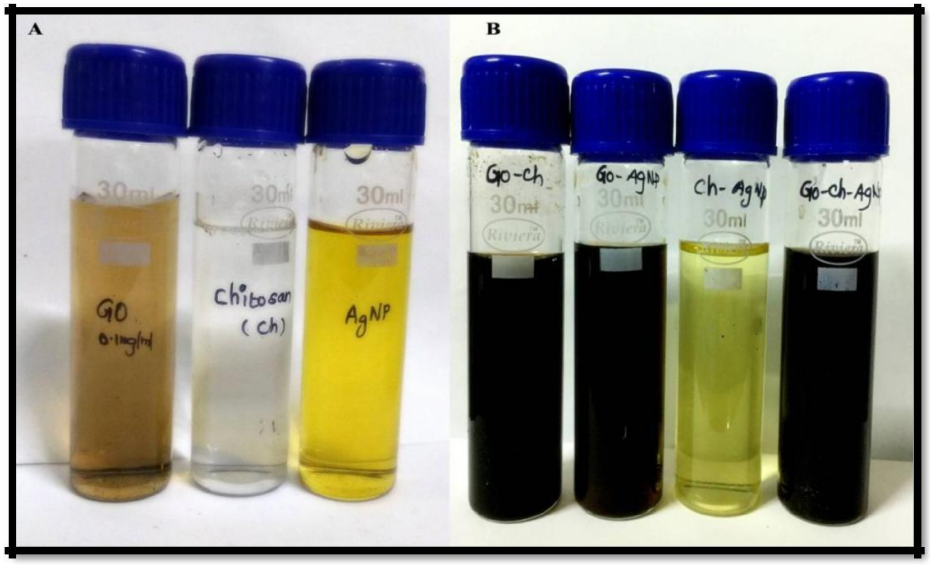

Figure 4.1: Photographic images of A) base components and B) composite solutions

4.2 Characterization of base and nanocomposites

4.2.1 Transmission Electron Microscopy analysis

The morphological aspects of GO nanosheets (GOns) and AgNPs were investigated by Transmission Electron Microscopy (TEM). Figure 4.2 A shows the TEM image of

transparent single layer GOns and Figure 4.2 B indicates the selected –area electron diffraction (SAED) pattern of GOns [44]. The hexagonal pattern indicates the single crystalline nature (001 plane) of the GO sheets formed. Figure 4.2 C shows the formation of monodispersed spherical silver nanoparticles of size around 10-15 nm [43]. The patterns of SAED (Figure 4.2 D) were indexed according to (111), (200), (220) and (311) reflections of FCC silver crystal which is consistent with the XRD pattern of silver nanoparticle.

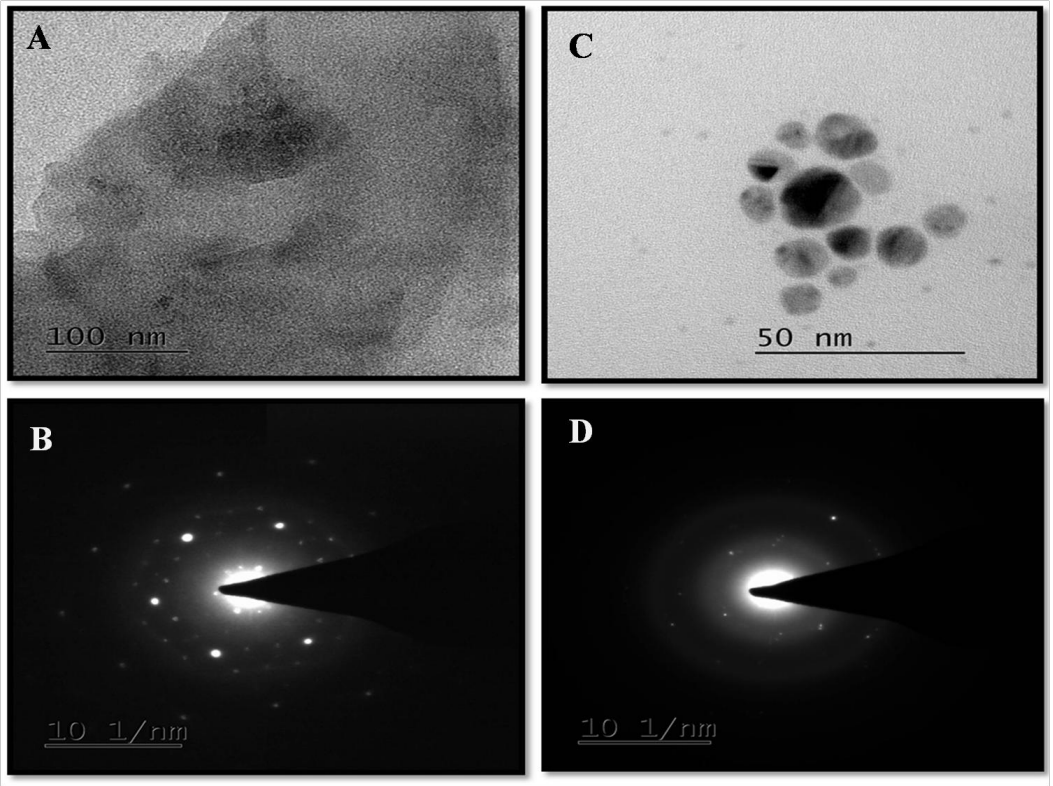

Figure 4.2: TEM images and SAED pattern of base components A, B) GO and C, D) AgNPs

4.2.2 UV-Visible spectroscopy

Figure 4.3 A illustrates the UV-Visible absorption spectra of the base components GOns, Chitosan and AgNPs. The black curve exhibited the spectrum of GOns has a sharp absorption peak at 230 nm and a shoulder peak at around 300 nm, which are attributed to $\pi - \pi^*$ transition of C=C bonds and n-π^* transition of C=O bonds, respectively. The peak of GOns is normally sharp and prominent at 230 nm for single layered GOns which is similar to peak already reported in the literature [45, 46]. The more $\pi - \pi^*$ transitions, the less energy needs to be used for the electronic transition, which results in a higher λ_{max}. The blue curve in the extinction spectra depicted a typical surface Plasmon resonance (SPR) band at 412 nm because of the collective oscillation of silver nanoparticles electron in resonance with the incident light wave which clearly indicates the formation of silver nanoparticles [43]. The smaller silver nanospheres primarily absorb light and have peaks near 400 nm, while

larger spheres exhibit increased scattering and have peaks that broaden and shift towards longer wavelengths (known as red-shifting). Hence, the peak at 412 nm suggested the formation of smaller AgNPs which was already confirmed by TEM analysis. The red curve of the absorption spectra exhibited an absorption band at 201 nm showed the presence of D-glucosamine units of chitosan. The AgNP dispersed nanocomposites showed absorption peak at 412 nm, 413 nm and 404 nm revealed the impregnation of AgNPs in GO (red curve), Ch (blue curve) and GO-Ch (green curve) colloidal solution is displayed in Figure 4.3 B [2]. However, 8 nm blue shift was occurred after the addition of chitosan to GO-Ch which is probably due to an etching process resulted in a small reduction in the size of AgNP. The black curve in the Figure 4.3 B showed two absorption peaks at 204 nm and 216 nm which are consistent with the base components absorption peak of Ch and GO solutions.

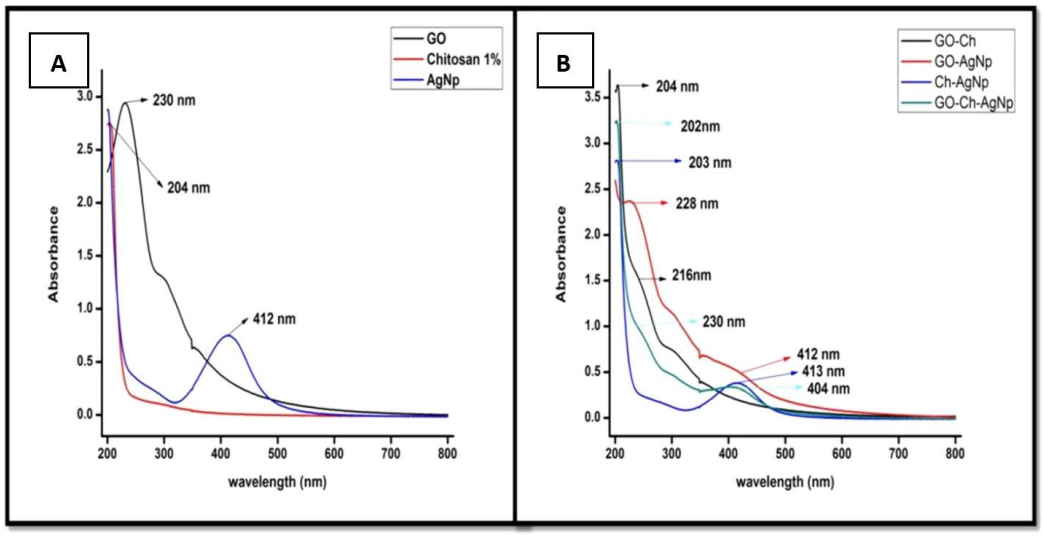

Figure 4.3: UV-vis absorption spectra of A) base components and B) composite colloids.

4.2.3 X-ray diffraction (XRD) analysis

X-ray diffractogram of the base and composite films are shown in the Figure 4.4. The GO film prepared by modified Hummer's method gives a characteristic peak around $2\theta = 8.81^{o}$ and the interlayer distance (d-spacing) were found to be 1.03 nm. The two-theta position (001) of the GO diffraction peak can show a range of 7-12º depending on the amount of residual water intercalated between basal planes in a GO film. The chitosan (Ch) film showed two characteristic reflections at 11.44º and 21.71º that are typical fingerprints of semi crystalline Chitosan indexed as (020) and (110) hydrated crystalline structure and an amorphous structure of chitosan, respectively. The XRD analysis of the Ag NPs showed peaks at 38.3º, 45.3º, 64.4º, and 77.95º are assigned to (111), (200), (220), and (311) crystallographic planes of face-centered cubic silver nanoparticles and it matched with the JCPDS silver file No. 04–0783 [47]. The GO-Ch composite showed peak at 9.15º (001)

and broadening of peak observed around $2\theta^0$ (110) confirmed the exfoliation of GO in the chitosan matrix. The GO-AgNP film showed broadened peak for 001 pattern of GO which clearly shows that the intercalation of silver nanoparticles in GO prevents the stacking of GO layers but the fcc planes of AgNP were clearly noticed. The silver nanoparticles immobilized in chitosan showed 111 plane of AgNP along with the 110 plane of Chitosan clearly exhibited the impregnation of AgNP in the chitosan matrix. The GO-Ch-AgNP film showed 001 plane of GO in addition to 110 and 111 plane of Chitosan and AgNPs [2].

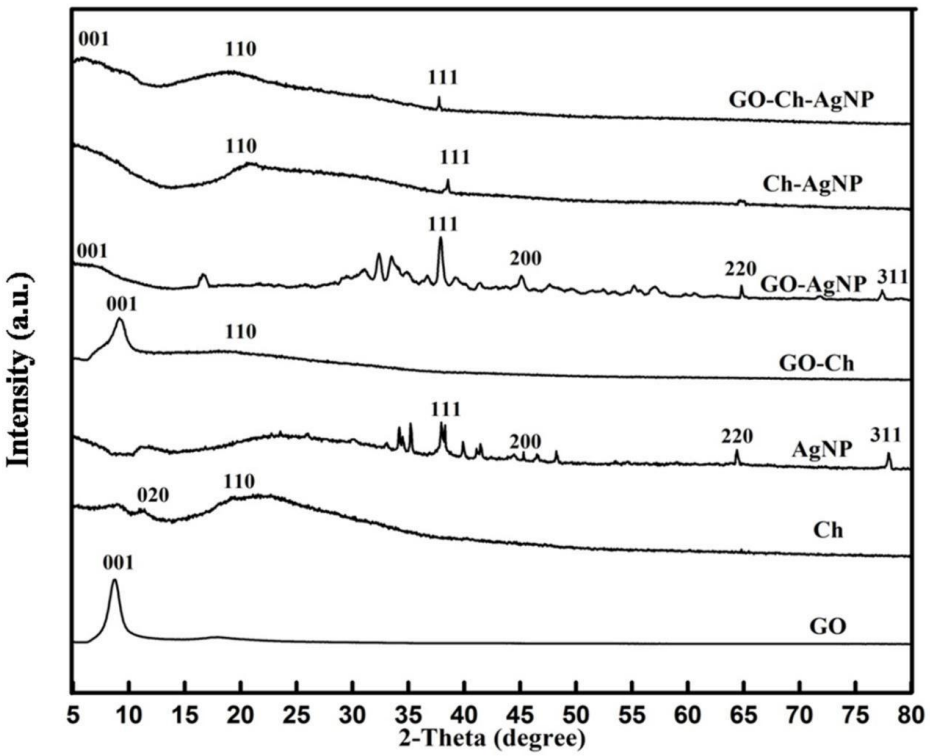

Figure 4.4: XRD Pattern of base component and composite film

4.2.4 FTIR analysis

The FT-IR spectrum of the base and composite films are illustrated in Figure 4.5 For GO, the an intense peak was observed at 3414 cm^{-1}, which is corresponded to the OH groups, and the strong peak at 1630 cm^{-1} related to the stretching vibrations of C=O carboxylic moieties. Other bands at 1400.84, 1227.49 and 1094 cm^{-1} related to C−O−H deformation, C−H stretching (epoxy groups), and C−O stretching vibrations (alkoxy groups), respectively. Therefore, it confirms the existences of the abundance of hydroxyl groups and oxygenous groups on the surface of GO [45]. The characteristic absorption bands for chitosan appeared at 3437.12 (O–H stretching vibrations), 2924 (C–H stretching vibrations), 1640 (N–H bending vibrations), 1415 (C– N stretching vibrations) and a band at 1076.44 cm^{-1} (C–O–C and C–O stretching vibrations). The characteristic band for AgNPs appeared at 3396 cm^{-1}

(O-H stretching), 2927 cm^{-1} and 1632 cm^{-1} (C-H stretching and O-H stretching attributed to the tightly bound water presented in the starch molecule),1384 cm^{-1} (C-H bending vibration),1154 cm^{-1}, 1080 cm^{-1} and 1023 cm^{-1} (C-O-C ether stretching vibration in glucose bonds, 577 cm^{-1} (C-H bending) [3]. In GO-Ch composite, the appearance of 2927 cm^{-1} (C-H stretching) of chitosan was noticed along with the other vibrations noticed in GO which confirmed the blending of Chitosan with GO. All the AgNP impregnated films showed C-H bending and C-O-C ether stretching observed in AgNP spectrum which confirmed the impregnation of AgNP in the composite. In GO-Ch-AgNP and Ch-AgNP composites showed characteristics C-H and C-N stretching observed in the spectrum of chitosan which further the presence of chitosan in the composite.

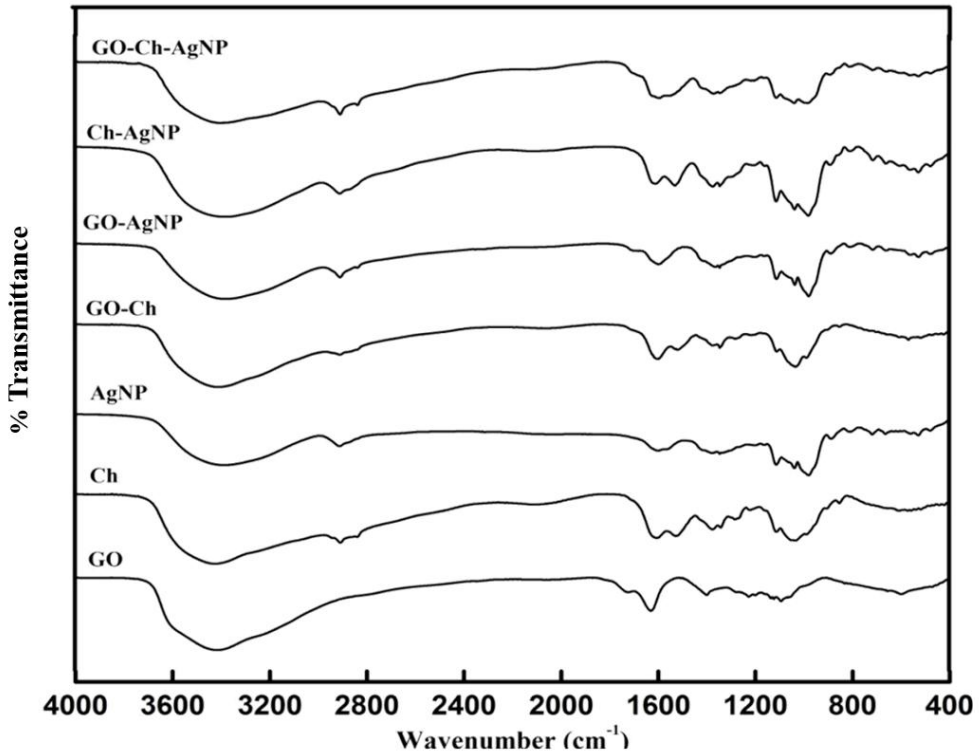

Figure 4.5: FT-IR spectrum analysis of base components and composites

4.2.5 Fabrication of composite films by drop casting method

The digital image of the prepared nanocomposites film is shown in the Figure 4.6. The films based on GO are black in color. Silver nanoparticles and chitosan were mixed with the GO and turned to black color .Chitosan- AgNP film looks yellow in color due to the mixing of AgNPs in the chitosan solution.

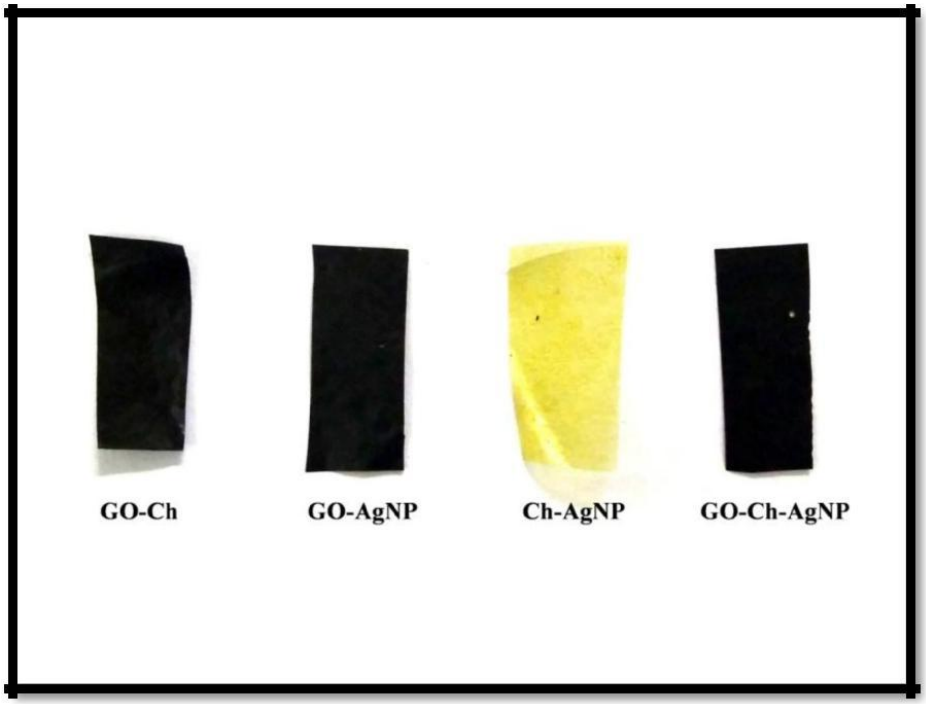

Figure 4.6: The photographic image of the composite films

4.2.6 FESEM analysis of composite films

The surface morphologies of the composite films were analyzed by FESEM and the images are shown in the Figure 4.7. In GO-Ch film (Figure 4.7 A), GO nanosheets dispersed uniformly in the chitosan matrix by the formation of amide linkages between GO and Chitosan [**?**] The aggregation of AgNPs over the chitosan matrix makes clumping of AgNPs over the surface (Figure 4.7 C). Unlike GO-Ch, numerous white spots were distributed on the surface of the GO-AgNP and GO-Ch-AgNP composites (Figure 4.7 B and D) [24].

4.2.7 Contact angle (CA) measurements

The surface hydrophobicity of the films was measured by the contact angle of water to the surface of the films and its plot is shown in the Figure 4.8. The GO-Ch composite exhibited the highest contact angle (106.55º) among the other composites due to the interaction between GO and Ch. Following GO-Ch, GO-Ch-AgNP and Ch-AgNP films showed hydrophobicity of 101.27º and 100.015º. The absence of chitosan made GO-AgNP film less hydrophobic 58.115º than others [44].

4.2.8 Tensile strength analysis

The mechanical properties of composite films were investigated by a universal testing machine at 18°C and their tensile strength is shown in the Figure 4.9. The strong amide linkages between carboxyl groups of GO and amine groups of chitosan resulted in significant

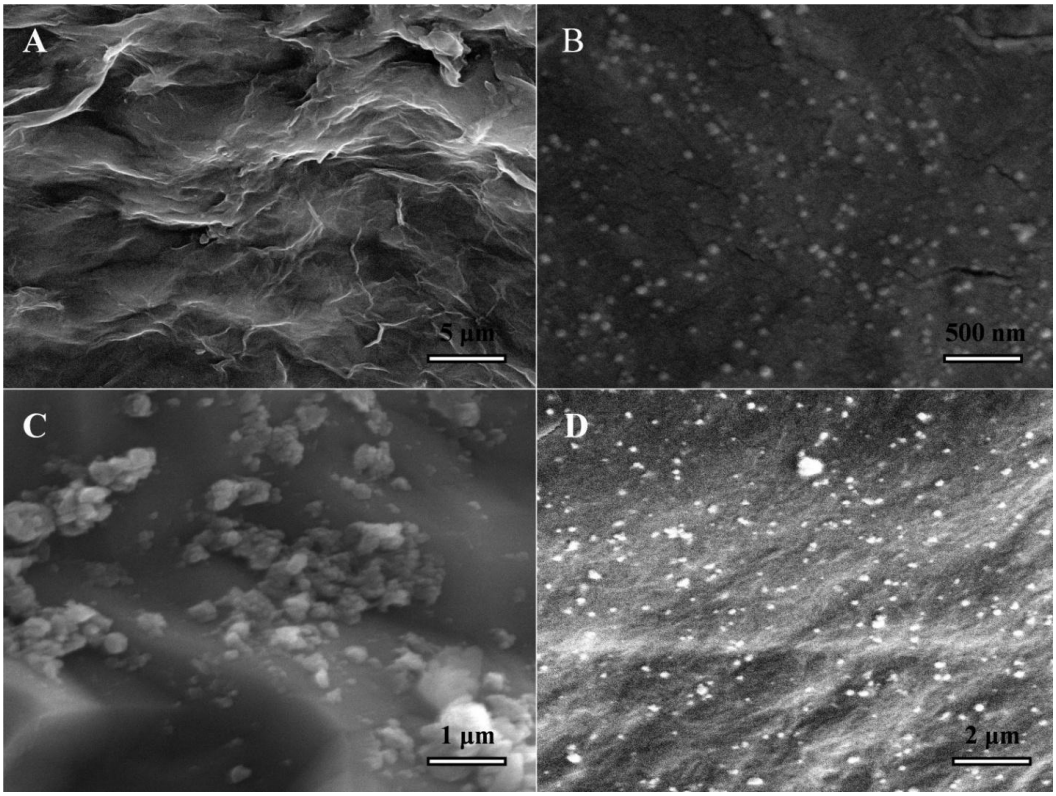

Figure 4.7: FESEM images of composite films A) GO-Ch, B) GO-AgNP, C) Ch-AgNP and D) GO-Ch-AgNP

increase in the tensile strength (163.04 MPa) of GO-Ch film [36]. The electrostatic interaction of silver ions with the oxygen functional group of GO is a weak attachment resulted in lower tensile strength (21.01 MPa) than others composites with chitosan. The AgNPs bind with the amine functional groups of chitosan resulted in better tensile strength (43.85 MPa) than GO-AgNP. In GO-Ch-AgNP film, AgNPs and GO compete to interact with amine oxygen functional groups of GO and functional groups Chitosan produces lesser tensile strength (27.175 MPa) composite than GO-Ch and Ch-AgNP film.

4.2.9 Degradation study of composite films

The degradation of the films over time is shown in the Figure 4.10. Due to its higher hydrophobicity and tensile strength GO-Ch film exhibits lesser degradation in the buffer even after 120 h of incubation it maintained stable film structure. The Ch-AgNP and GO-AgNP films almost degrading in the similar rate but Ch-AgNP film expands in aqueous buffer. The GO-Ch-AgNP film degrades little faster than others because of the less amount of chitosan present. But all the films maintain almost 90% of its weight. We can increase the stability of the films by increasing the concentration of chitosan. Because longer stability can make it as a promising coating material.

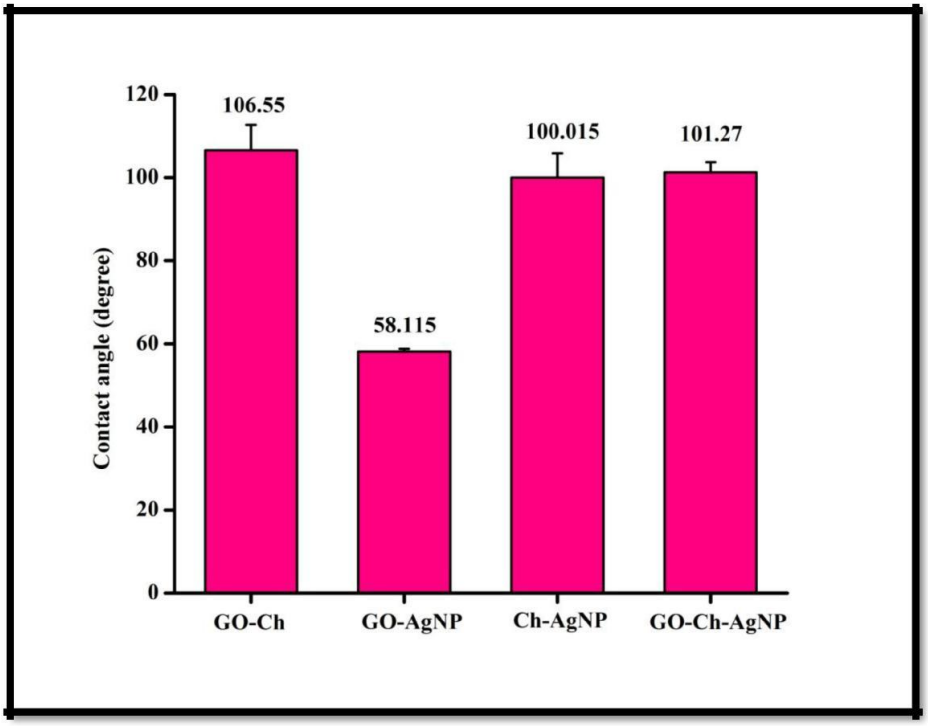

Figure 4.8: Contact angle measurement of the composite films

4.2.10 Study on leaching of silver from the composites

The UV-vis spectra shown in the Figure 4.11 showed no peak in the range of 400- 420 nm revealed that there is no leaching of AgNPs in to the water medium. Due to its interaction with the oxygen and amide group of GO and Ch it is completely immobilized over the surface resulted in zero leaching of particles [32]. The immobilized AgNPs are capable of capture killing the bacteria when attached to the surface. Also, AgNP immobilized films serves as long term reservoir of AgNPs with enhanced activity.

4.3 Antibiofilm activity of the films

4.3.1 Effectiveness of composites films tested by zone of inhibition (ZOI) plate assay

The antibacterial activity of the composite films was tested against *E.coli* Figure 4.12 (A-C) and *B.subtilis* Figure 4.12 (D-E) by zone of inhibition assay and the photographs are shown in Figure 4.12. The control images Figure 4.12 (A and D) displayed the growth of bacteria all over the plate whereas all the composites (B, C, E and F) showed contact area inhibition against the test bacteria. A little zone of clearance was noticed surrounding the AgNP impregnated films against *E.coli* [24, 26]. But no such zone was observed surrounding the AgNP impregnated films against *B.subtilis*. This may be due to the thicker peptidoglycan

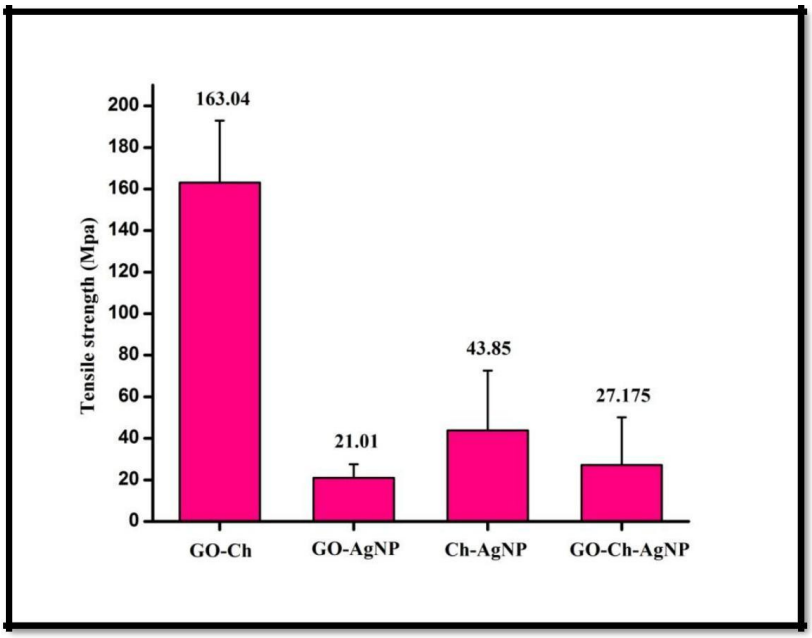

Figure 4.9: Tensile strength analysis of the composites

layer of Gram positive bacteria *B.subtilis* The electrostatic interaction between the bacterial cell wall and the nanoparticle or chitosan makes results in the cell wall disruptions [20, 21]. Once again it is proved that gram negative bacteria are more susceptible than gram positive.

4.3.2 Effectiveness of films over fimbriae production on congo red agar plate

The morphology of the colonies formed by *E.coli* and *B.subtilis* on Congo red plates after 48 h of incubation were photographed and shown in Figure 4.13 and 4.14. The morphology of the colony produced over congo red control plate without film (Figure 4.13 A and 4.14 A) showed rugose pink colony structure which is similar to Extracellular Polymeric Substances (EPS) production where as no growth of bacteria was observed over composite films shown in Figure 4.13 and 4.14 (B-E). The pink color appearance of the colony is due to the absorption of Congo red in the agar by the polysaccharide produced in the EPS matrix [48].

The AgNP containing composites in Figure 4.13 and 4.14 (C-E) showed no colony formation over and surrounding the films. Due to the presence of AgNP the bacteria were killed and no longer available to form colonies this clearly indicates capture killing process of silver nanoparticles immobilized over the films [24]. On the other hand, GO-Ch film in Figure 4.13 and 4.14 (B) showed white colony formation surrounding the film due to lack of AgNP it was not able to kill the bacteria. The white colony suggested that the bacterium grown doesn't form biofilm and could not able to absorb congo red from the agar. This clearly explains that the surface of the film is hydrophobic over which attachment is lesser possible thereby preventing the formation of biofilms over the surface [49].

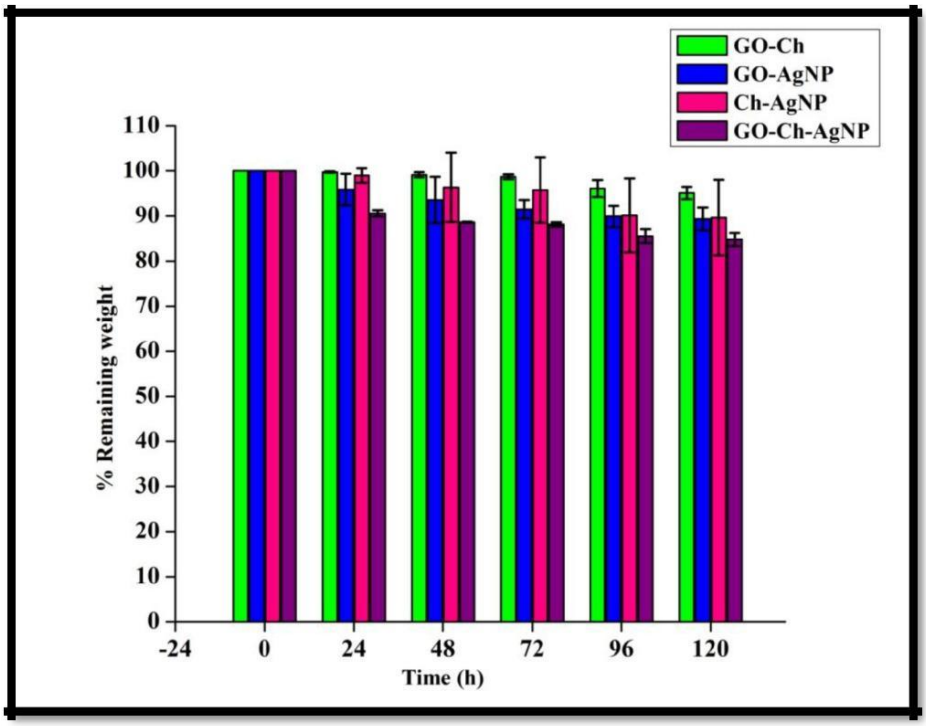

Figure 4.10: Degradation of composites over time

4.3.3 Swarming motility assay

The swarming motility of *E.coli* and *B.subtilis* was evaluated in the presence of the films were assayed and photographed in the Figure 4.15 and 4.16. In the control (Figure 4.15 and 4.16 A) both the bacteria formed dendrite swarm pattern on swarm agar plates. The bacteria swarm with the help of large number of pilus surrounding the surface. Biofilm forming bacteria produces more number of pilus and helps the bacteria to move over the surface to form a conditioning layer which is the first step of biofilm formation [50]. The swarm pattern confirmed the ability of the bacteria to form biofilm over the agar surface provided with nutrient.

But no swarm pattern was observed over any film surface in Figure 4.15 and 4.16 (B-E).The absence of AgNP in GO-Ch film in Figure 4.15 and 4.16 (B) promotes swarming surrounding the surface of the film but its hydrophobic nature doesn't allow bacteria to swarm on it. The silver nanoparticle impregnated films in Figure 4.15 and 4.16 (C-E) kills the bacteria on its surface and thereby prevents swarming of bacteria around the film [26]. But bacteria escaped from the contact of AgNP showed lesser swarm pattern compared to control and GO-Ch. This again confirmed the contact killing property of AgNPs and Surface hydrophobicity of GO-Ch films.

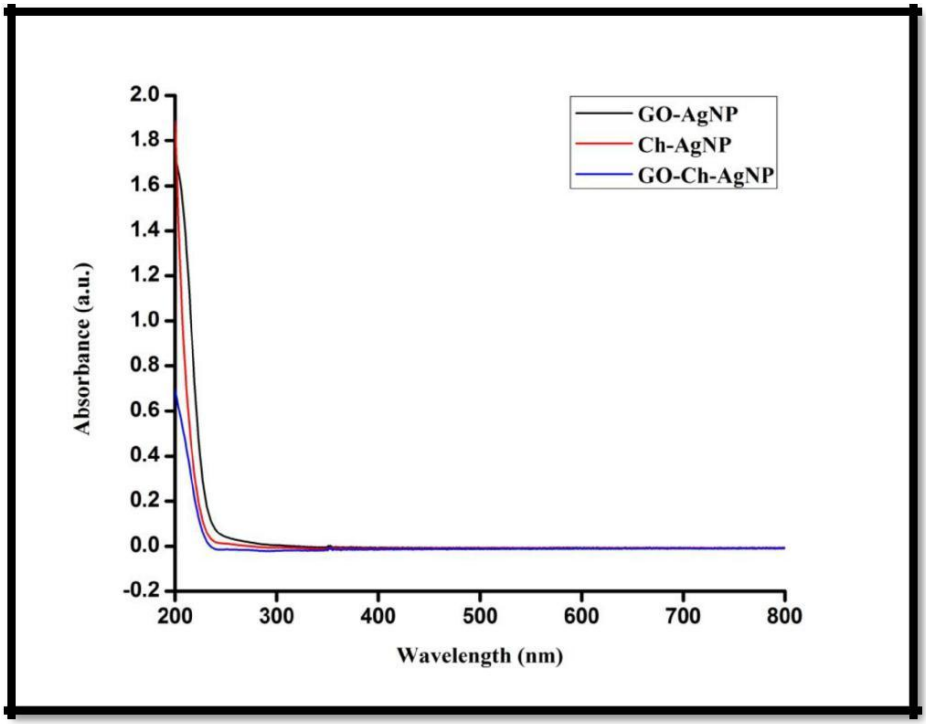

Figure 4.11: Leaching study of silver from composites.

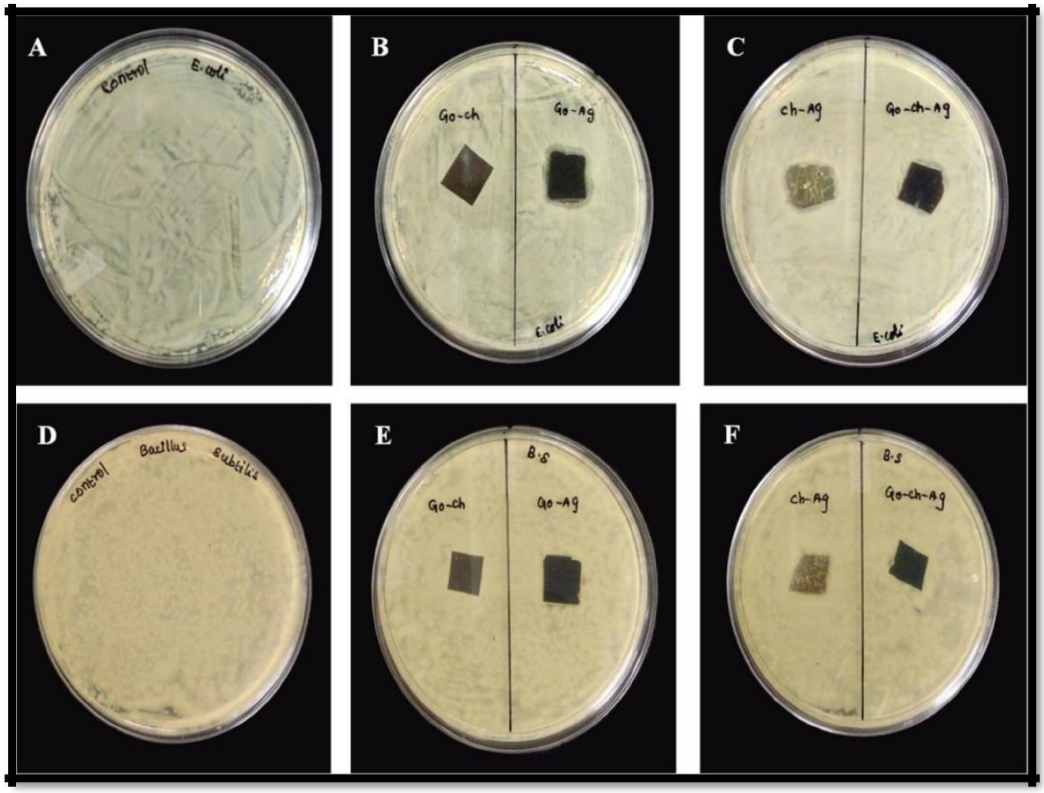

Figure 4.12: Zone of inhibition assay against *E.coli* (A-C) and *Bacillus subtilis* (D-F)

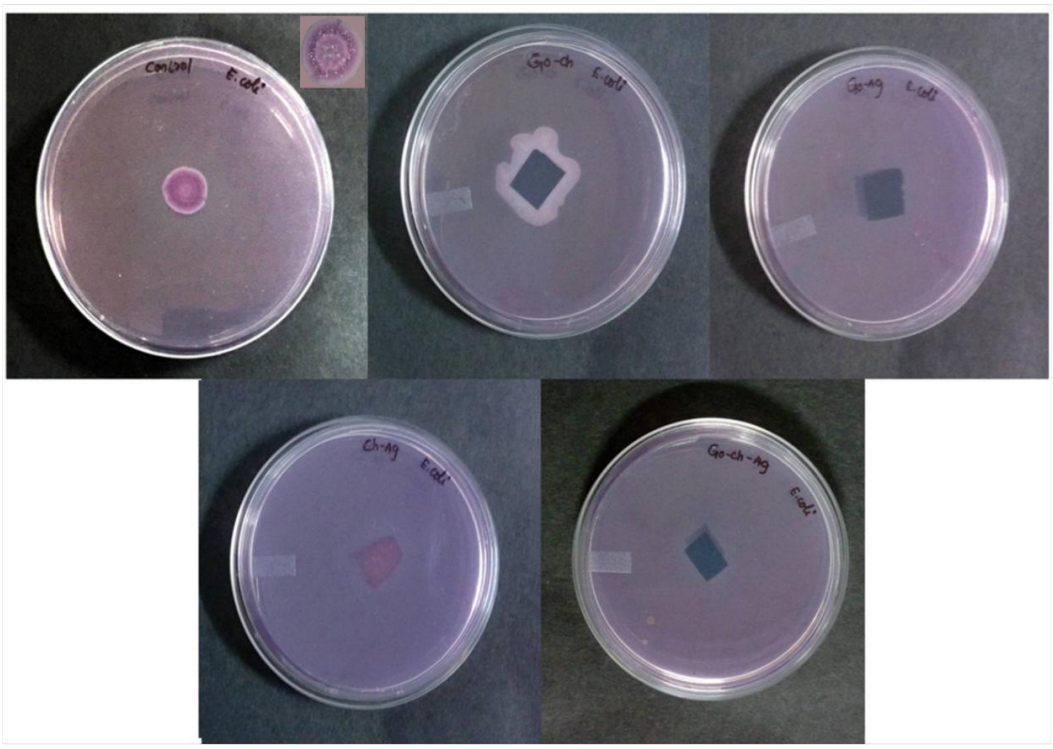

Figure 4.13: Fimbriae production analysis by colony morphology assay against *E.coli.* A) Control, B) GO-Ch , C) GO-AgNP, D) Ch-AgNP and E) GO-Ch-AgNP film

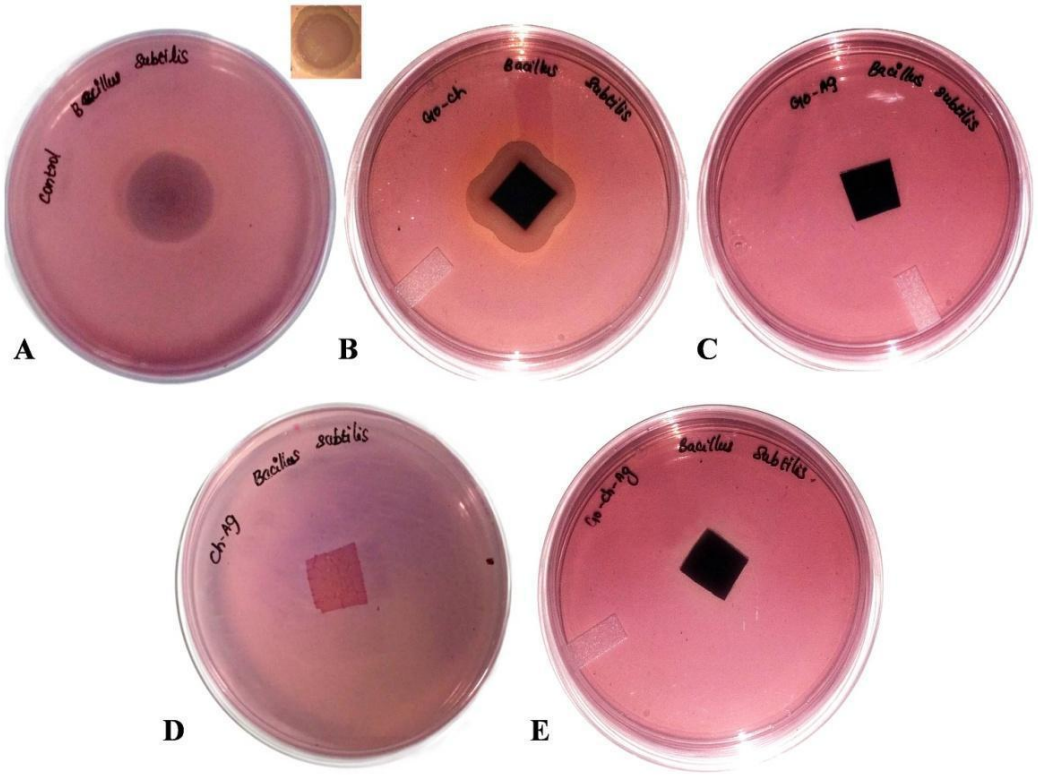

Figure 4.14: Fimbriae production analysis by colony morphology assay against *Bacillus subtilis.* A) Control, B) GO-Ch , C) GO-AgNP, D) Ch-AgNP and E) GO-Ch-AgNP film

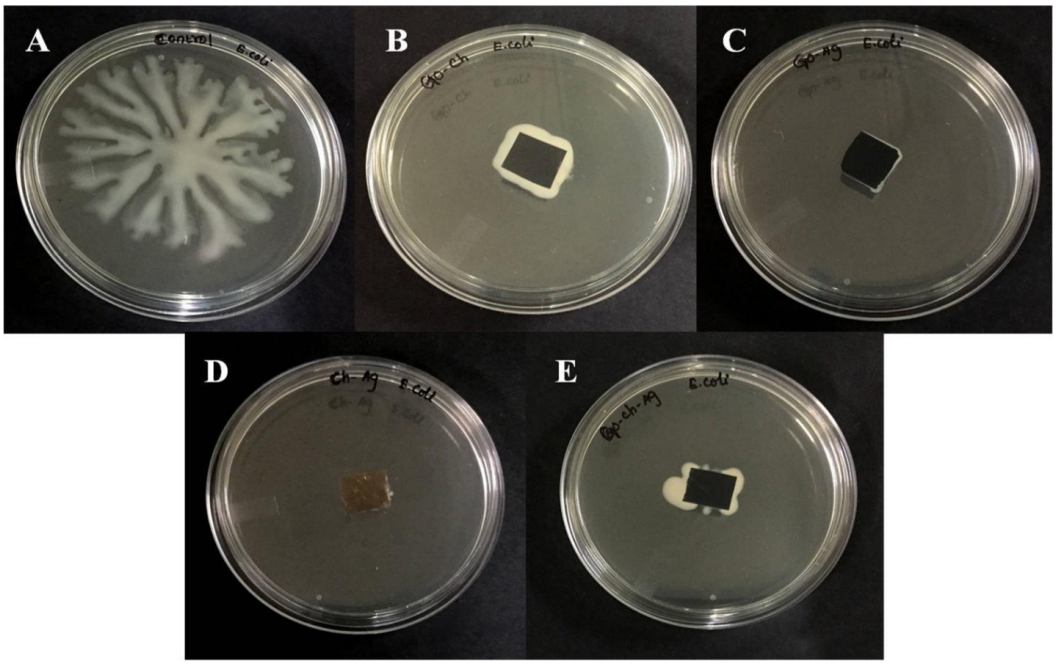

Figure 4.15: Swarm pattern analysis by swarming motility assay against *E.coli.* A) Control, B) GO-Ch , C) GO-AgNP, D) Ch-AgNP and E) GO-Ch-AgNP film

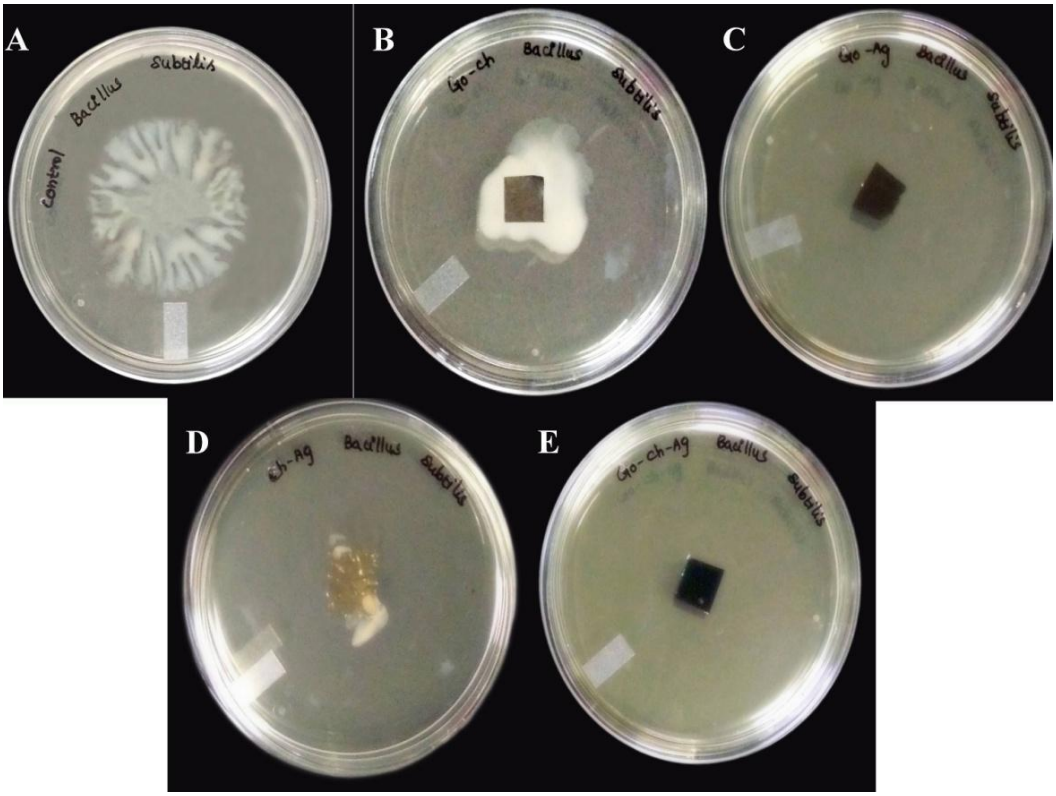

Figure 4.16: Swarming pattern analysis by swarming motility assay against *Bacillus subtilis.* A) Control, B) GO-Ch , C) GO-AgNP, D) Ch-AgNP and E) GO-Ch-AgNP film

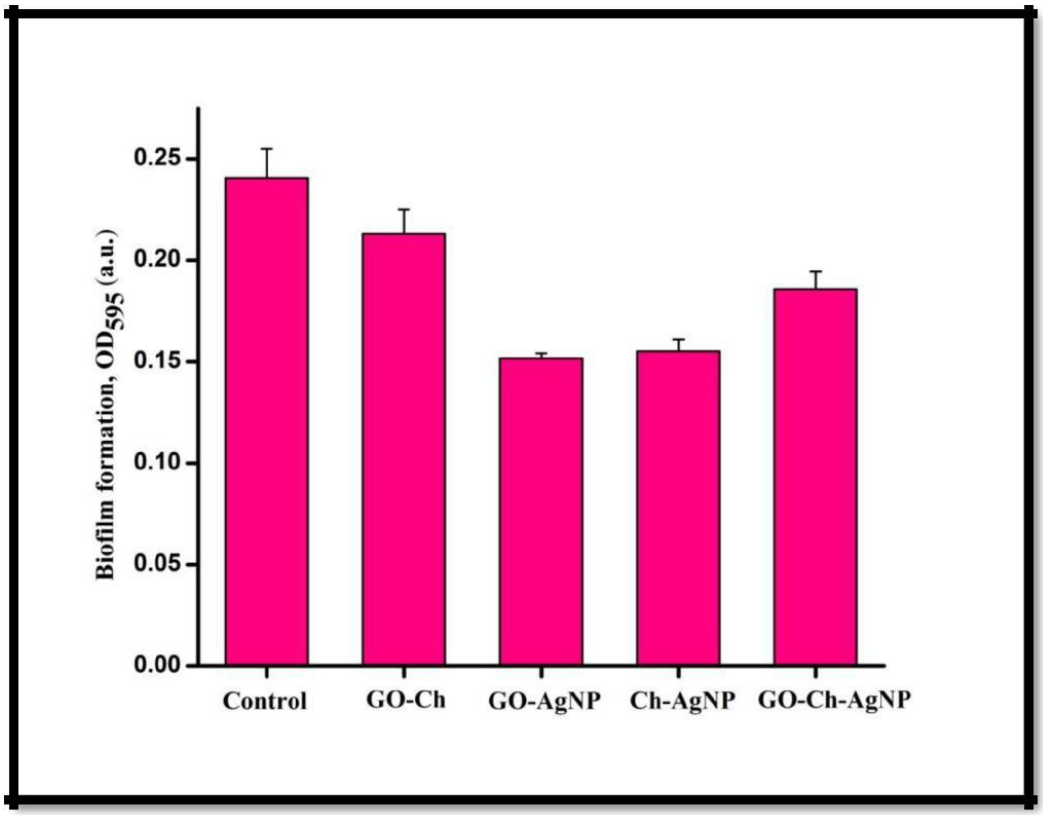

Figure 4.17: Quantification of biofilm formation by *E.coli* on the walls of test tubes with the presence of nanocomposite

4.3.4 Biofilm static assay

This indirect biofilm formation measurement assay quantified the amount of biofilm formation in the presence of various composites against *E.coli* and *B.subtilis* is shown in Figure 4.17 and 4.19. The photographed image of the crystal violet stained biofilm over the surface of the test tubes are shown in Figure 4.18 and 4.20. The biofilm formation was quantified more in the control compared to all the composites [51]. The GO-Ch film allows lesser attachment of bacteria over the surface hence bacteria started forming biofilm on the test tube walls. Even though the amount of biofilm formation is almost equal to the control, the reduction in biofilm formation may be due to the killing of bacteria by the sharp edges of GO. The GO-Ch-AgNP film is also hydrophobic leads to lesser attachment of bacteria over the film but killing of bacteria due to the presence of AgNP made lesser biofilm formation compared to GO-Ch. The other two composites GO-AgNP and Ch-AgNP killed bacteria due to the presence of more AgNP resulted in the reduction of biofilm formation.

4.3.5 FESEM analysis of attachment of bacteria over composite films

The biofilm formation and bacterial morphology of *E.coli* and *B. subtilis* over the surface of the films were analyzed by Field Emission Scanning Electron Microscopy is shown in

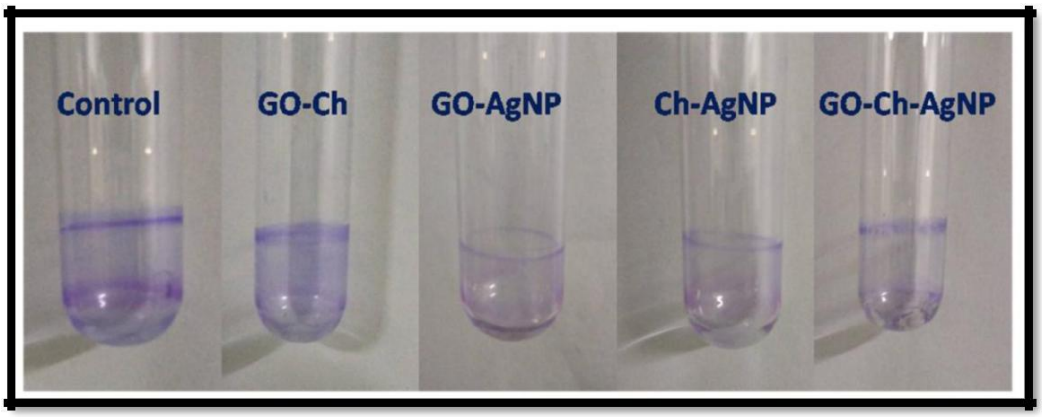

Figure 4.18: The photographic image of the biofilm formed on the test tube walls by *E.coli* stained with crystal violet dye

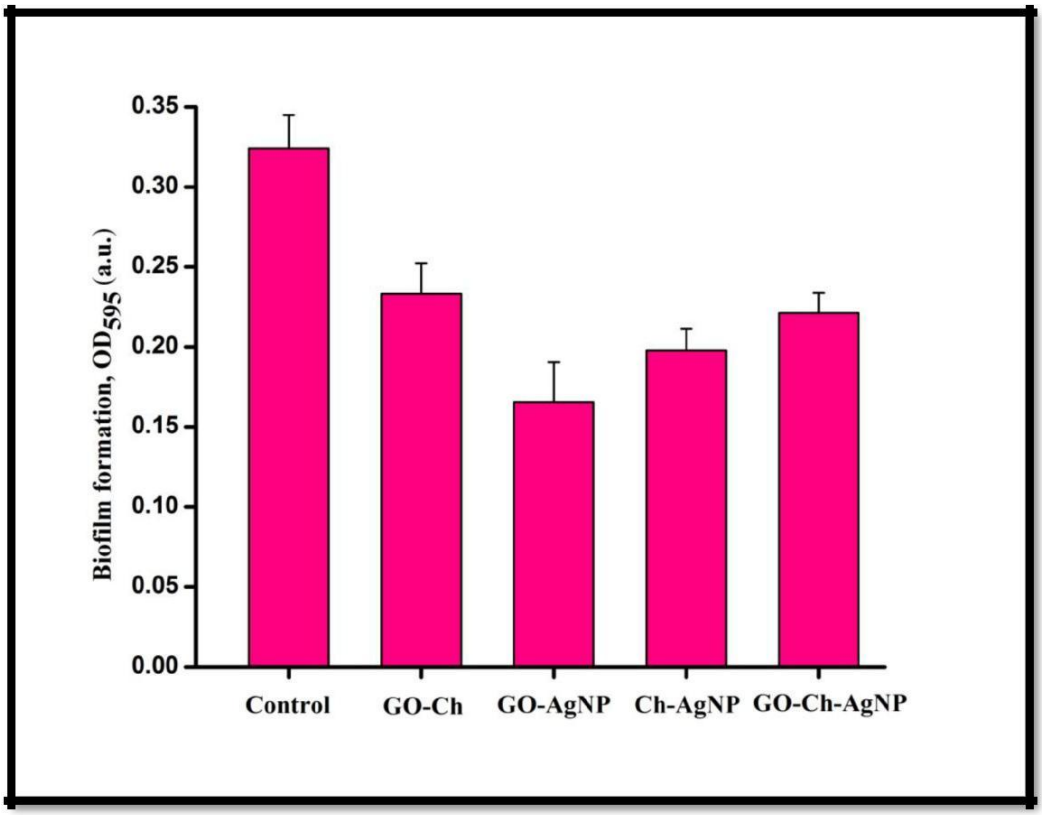

Figure 4.19: Quantification of biofilm formation by *Bacillus subtilis* on the walls of test tubes with the presence of nanocomposite

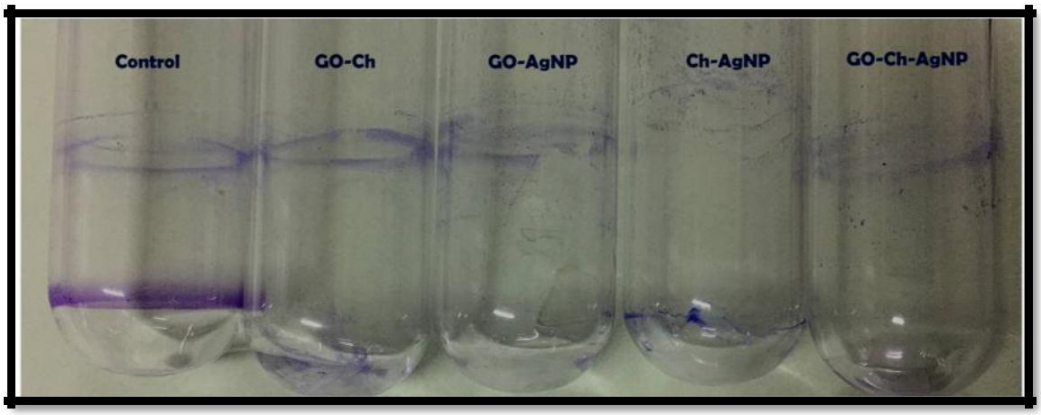

Figure 4.20: The photographic image of the biofilm formed on the test tube walls by *Bacillus subtilis* stained with crystal violet dye

the Figure 4.21 and 4.22. The control image (Figure 4.21 and 4.22 A) clearly showed the clump of bacteria connected by network whereas no clumping and biofilm formation were observed over the surface of the films in Figure 4.21 and 4.22 (B-E). The GO-Ch film in Figure 4.21 and 4.22 (B) showed the individual attachment of bacteria on its surface whereas AgNP impregnated films in Figure 4.21 and 4.22 (C-E) showed silver nanoparticles inside the bacterial cells [52].

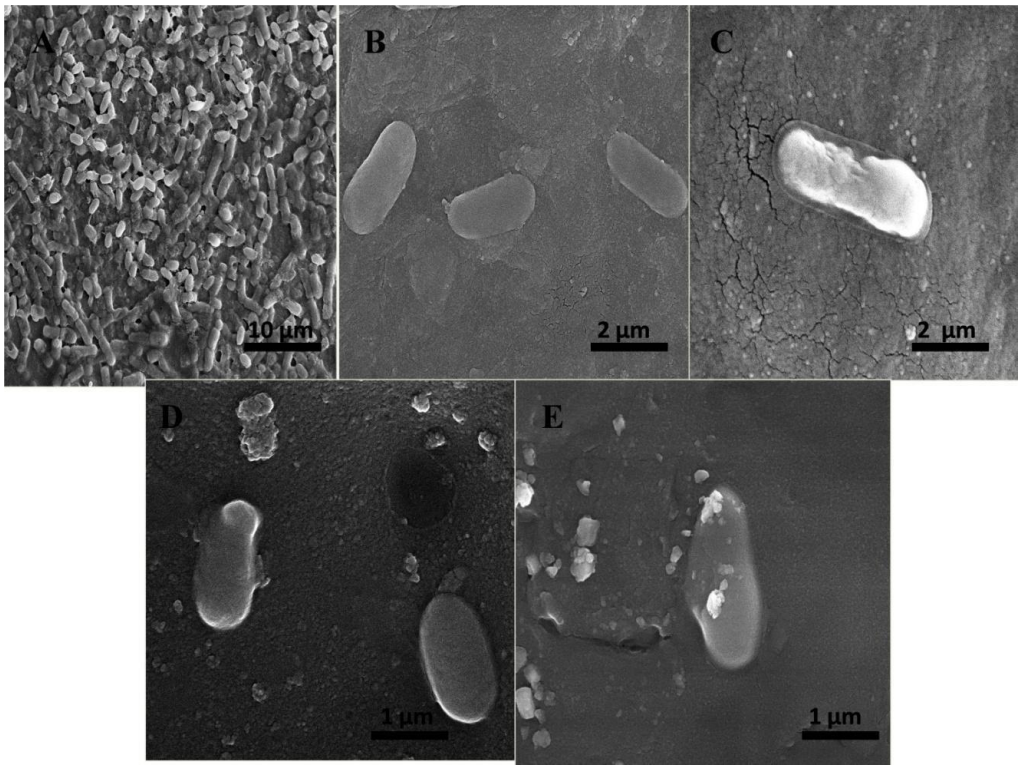

Figure 4.21: FESEM images of *E.coli* bacteria attached over A) Control surface B) GO-Ch film, C) GO-AgNP film, D) Ch-AgNP film and E) GO-Ch-AgNP film

The morphological changes such as distortion of cell wall was observed more in the

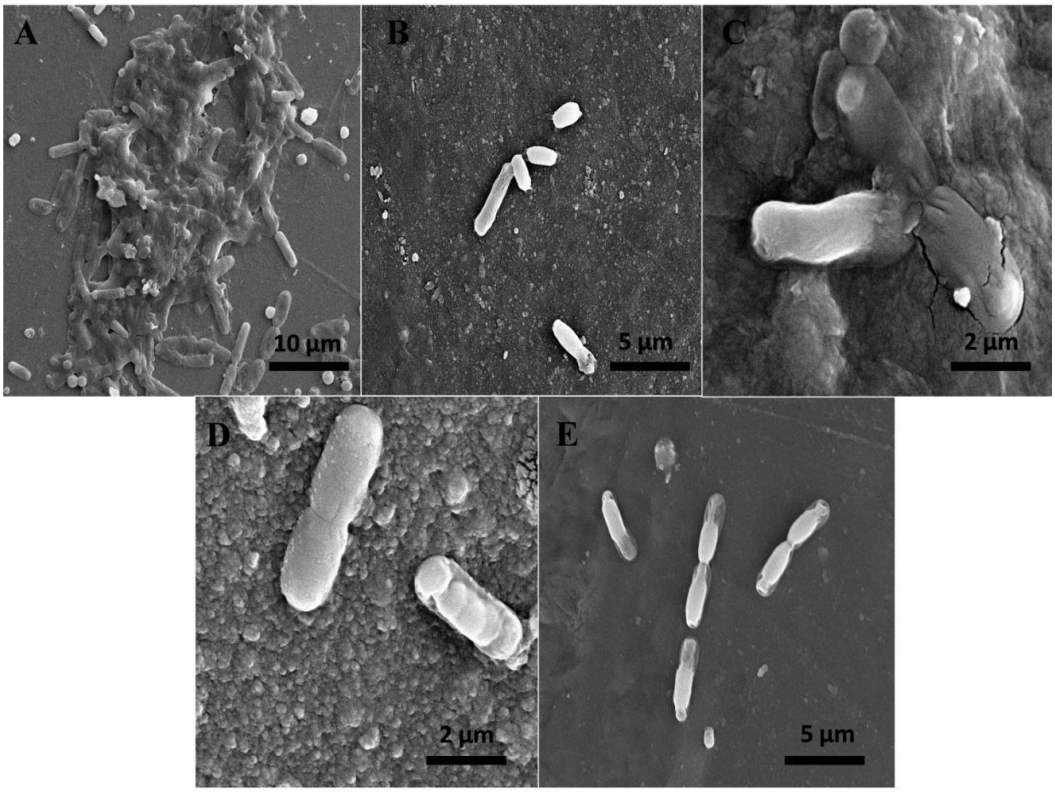

Figure 4.22: FESEM images of *Bacillus subtilis* bacteria attached over A) Control surface B) GO-Ch film, C) GO-AgNP film, D) Ch-AgNP film and E) GO-Ch-AgNP film

gram negative bacteria *E.coli* because of its thin peptidoglycan layer whereas AgNPs were attached over cell wall of *B. subtilis* because its thick peptidoglycan layer doesn't allow more AgNPs to penetrate thereby lesser distortion of bacteria was observed compared to *E.coli* [3].

Chapter 5

Conclusion

In summary, composite films were fabricated by facile and an environmentally friendly method. Moreover, starch capping prevented the agglomeration of AgNPs and the particles were well dispersed on the surface of GO and Chitosan. The anti-biofilm activity of the composite films was checked against Gram-negative bacterial strain *Escherichia coli* and Gram - positive bacterial strain *Bacillus subtilis*. The plate assays confirmed that all the composites exhibited contact area inhibition and the growth of bacteria was noticed surrounding the GO-Ch film in contrast little or no growth was observed surrounding the AgNP impregnated film which clearly explains AgNP plays an important role in killing of bacteria. The anti- adhesion is a key factor in the prevention of biofilm formation. Out of all the composites prepared, GO-Ch showed higher hydrophobicity compared to others which exhibited lesser attachment of bacteria on its surface but no killing of bacteria was noticed. All other AgNP impregnated composites exhibited antibacterial activity through contact killing process by AgNPs. Even though all the AgNP impregnated films exhibited anti-bacterial activity, GO-AgNP showed lesser hydrophobicity and lower tensile strength. The brittle nature of the film makes it less effective as a coating material. On the other hand, hydrophobic Ch-AgNP film was structurally unstable. The absence of GO makes the film shrinks when exposed to aqueous media. Hence, GO-Ch-AgNP composite contribute anti-bacterial and anti-adhesion properties in a synergistic manner will be the promising coating material as biocidal paints, glass coatings in various domestic and industrial settings.

Bibliography

[1] Shariq Qayyum and Asad U Khan. Nanoparticles vs. biofilms: a battle against another paradigm of antibiotic resistance. MedChemComm, 7(8):1479–1498, 2016.

[2] Andreia Fonseca de Faria, Diego Stéfani Teodoro Martinez, Stela Maris Meister Meira, Ana Carolina Mazarin de Moraes, Adriano Brandelli, Antonio Gomes Souza Filho, and Oswaldo Luiz Alves. Anti-adhesion and antibacterial activity of silver nanoparticles supported on graphene oxide sheets. Colloids and Surfaces B: Biointerfaces, 113: 115–124, 2014.

[3] Wei Shao, Xiufeng Liu, Huihua Min, Guanghui Dong, Qingyuan Feng, and Songlin Zuo. Preparation, characterization, and antibacterial activity of silver nanoparticle-decorated graphene oxide nanocomposite. ACS applied materials & interfaces, 7(12):6966–6973, 2015.

[4] Rob Van Houdt and Chris W Michiels. Biofilm formation and the food industry, a focus on the bacterial outer surface. Journal of applied microbiology, 109(4):1117–1131, 2010.

[5] M Monte-Serrano, P Fernandez-Saiz, R M Ortí-Lucas, and B Hernando. Effective Antimicrobial Coatings Containing Silver-Based Nanoclays and Zinc Pyrithione. Journal of Microbial and Biochemical Technology, 7:398–403, 2015.

[6] M Cloutier, D Mantovani, and F Rosei. Antibacterial coatings: challenges, perspectives, and opportunities. Trends in biotechnology, 33(11):637–652, 2015.

[7] Roya Dastjerdi and Majid Montazer. A review on the application of inorganic nano-structured materials in the modification of textiles: focus on anti-microbial properties. Colloids and Surfaces B: Biointerfaces, 79(1):5–18, 2010.

[8] Jayesh P Ruparelia, Arup Kumar Chatterjee, Siddhartha P Duttagupta, and Suparna Mukherji. Strain specificity in antimicrobial activity of silver and copper nanoparticles. Acta biomaterialia, 4(3):707–716, 2008.

[9] Michał Moritz and Małgorzata Geszke-Moritz. The newest achievements in synthesis, immobilization and practical applications of antibacterial nanoparticles. Chemical Engineering Journal, 228:596–613, 2013.

[10] Nicolas Barraud, Daniel J Hassett, Sung-Hei Hwang, Scott A Rice, Staffan Kjelleberg, and Jeremy S Webb. Involvement of nitric oxide in biofilm dispersal of Pseudomonas aeruginosa. Journal of bacteriology, 188(21):7344–7353, 2006.

[11] Megha Upadya, Annie Shrestha, and Anil Kishen. Role of efflux pump inhibitors on the antibiofilm efficacy of calcium hydroxide, chitosan nanoparticles, and light-activated disinfection. Journal of endodontics, 37(10):1422–1426, 2011.

[12] Angelo Taglietti, Yuri A Diaz Fernandez, Elvio Amato, Lucia Cucca, Giacomo Dacarro, Pietro Grisoli, Vittorio Necchi, Piersandro Pallavicini, Luca Pasotti, and Maddalena Patrini. Antibacterial activity of glutathione-coated silver nanoparticles against gram positive and gram negative bacteria. Langmuir, 28(21):8140–8148, 2012.

[13] Xiansong Wang, Peng Huang, Lili Feng, Meng He, Shouwu Guo, Guangxia Shen, and Daxiang Cui. Green controllable synthesis of silver nanomaterials on graphene oxide sheets via spontaneous reduction. Rsc Advances, 2(9):3816–3822, 2012.

[14] Sasha Stankovich, Dmitriy A Dikin, Richard D Piner, Kevin A Kohlhaas, Alfred Kleinhammes, Yuanyuan Jia, Yue Wu, SonBinh T Nguyen, and Rodney S Ruoff. Synthesis of graphene-based nanosheets via chemical reduction of exfoliated graphite oxide. carbon, 45(7):1558–1565, 2007.

[15] Kinga Haubner, Jan Murawski, Phillip Olk, Lukas M Eng, Christoph Ziegler, Barbara Adolphi, and Evelin Jaehne. The route to functional graphene oxide. ChemPhysChem, 11(10):2131–2139, 2010.

[16] Wenbing Hu, Cheng Peng, Weijie Luo, Min Lv, Xiaoming Li, Di Li, Qing Huang, and Chunhai Fan. Graphene-based antibacterial paper. ACS nano, 4(7):4317–4323, 2010.

[17] Renu Pasricha, Shweta Gupta, and Avanish Kumar Srivastava. A Facile and Novel Synthesis of Ag–Graphene-Based Nanocomposites. Small, 5(20):2253–2259, 2009.

[18] Lei Liu, Jincheng Liu, Yinjie Wang, Xiaoli Yan, and Darren Delai Sun. Facile synthesis of monodispersed silver nanoparticles on graphene oxide sheets with enhanced antibacterial activity. New Journal of Chemistry, 35(7):1418–1423, 2011.

[19] Manash R Das, Rupak K Sarma, Ratul Saikia, Vinayak S Kale, Manjusha V Shelke, and Pinaki Sengupta. Synthesis of silver nanoparticles in an aqueous suspension of graphene oxide sheets and its antimicrobial activity. Colloids and Surfaces B: Biointerfaces, 83(1):16–22, 2011.

[20] Rejane C Goy, Sinara T B Morais, and Odilio B G Assis. Evaluation of the antimicrobial activity of chitosan and its quaternized derivative on E. coli and S. aureus growth. Revista Brasileira de Farmacognosia, 26(1):122–127, 2016.

[21] Pallab Sanpui, A Murugadoss, P V Durga Prasad, Siddhartha Sankar Ghosh, and Arun Chattopadhyay. The antibacterial properties of a novel chitosan–Ag-nanoparticle composite. International journal of food microbiology, 124(2):142–146, 2008.

[22] Jianghu Cui, Chaofan Hu, Yunhua Yang, Yongjian Wu, Lufeng Yang, Yaling Wang, Yingliang Liu, and Zhenyou Jiang. Facile fabrication of carbonaceous nanospheres loaded with silver nanoparticles as antibacterial materials. Journal of Materials Chemistry, 22(16):8121–8126, 2012.

[23] Enrique Navarro, Flavio Piccapietra, Bettina Wagner, Fabio Marconi, Ralf Kaegi, Niksa Odzak, Laura Sigg, and Renata Behra. Toxicity of silver nanoparticles to Chlamydomonas reinhardtii. Environmental science & technology, 42(23):8959–8964, 2008.

[24] Jun Sung Kim, Eunye Kuk, Kyeong Nam Yu, Jong-Ho Kim, Sung Jin Park, Hu Jang Lee, So Hyun Kim, Young Kyung Park, Yong Ho Park, and Cheol-Yong Hwang. Antimicrobial effects of silver nanoparticles. Nanomedicine: Nanotechnology, Biology and Medicine, 3(1):95–101, 2007.

[25] H Le Pape, F Solano-Serena, P Contini, C Devillers, Abderrahman Maftah, and P Leprat. Involvement of reactive oxygen species in the bactericidal activity of activated carbon fibre supporting silver: Bactericidal activity of ACF (Ag) mediated by ROS. Journal of inorganic biochemistry, 98(6):1054–1060, 2004.

[26] A Dror-Ehre, H Mamane, T Belenkova, G Markovich, and A Adin. Silver nanoparticle–E. coli colloidal interaction in water and effect on E. coli survival. Journal of Colloid and Interface Science, 339(2):521–526, 2009.

[27] Chun-Nam Lok, Chi-Ming Ho, Rong Chen, Qing-Yu He, Wing-Yiu Yu, Hongzhe Sun, Paul Kwong-Hang Tam, Jen-Fu Chiu, and Chi-Ming Che. Silver nanoparticles: partial oxidation and antibacterial activities. JBIC Journal of Biological Inorganic Chemistry, 12(4):527–534, 2007.

[28] Aleš Panáček, Libor Kvítek, Robert Prucek, Milan Kolář, Renata Večeřová, Naděžda Pizúrová, Virender K Sharma, Tat ‘jana Nevěčná, and Radek Zbořil. Silver colloid nanoparticles: synthesis, characterization, and their antibacterial activity. The Journal of Physical Chemistry B, 110(33):16248–16253, 2006.

[29] Sukdeb Pal, Yu Kyung Tak, and Joon Myong Song. Does the antibacterial activity of silver nanoparticles depend on the shape of the nanoparticle? A study of the gram-negative bacterium Escherichia coli. Applied and environmental microbiology, 73(6):1712–1720, 2007.

[30] Justin T Seil and Thomas J Webster. Antimicrobial applications of nanotechnology: methods and literature. Int J Nanomedicine, 7:2767–2781, 2012.

[31] Hui Yang, Yan Liu, Qianhong Shen, Liangfu Chen, Wenhui You, Xinmin Wang, and Jiansong Sheng. Mesoporous silica microcapsule-supported Ag nanoparticles fabricated via nano-assembly and its antibacterial properties. Journal of Materials Chemistry, 22(45):24132–24138, 2012.

[32] Xiaoming Yang, Yingfeng Tu, Liang Li, Songmin Shang, and Xiao-ming Tao. Well-dispersed chitosan/graphene oxide nanocomposites. ACS applied materials & interfaces, 2(6):1707–1713, 2010.

[33] Entsar I Rabea, Mohamed E-T Badawy, Christian V Stevens, Guy Smagghe, and Walter Steurbaut. Chitosan as antimicrobial agent: applications and mode of action. Biomacromolecules, 4(6):1457–1465, 2003.

[34] Dongwei Wei, Wuyong Sun, Weiping Qian, Yongzhong Ye, and Xiaoyuan Ma. The synthesis of chitosan-based silver nanoparticles and their antibacterial activity. Carbohydrate research, 344(17):2375–2382, 2009.

[35] Xin Zhao, Qinghua Zhang, Dajun Chen, and Ping Lu. Enhanced mechanical properties of graphene-based poly (vinyl alcohol) composites. Macromolecules, 43 (5):2357–2363, 2010.

[36] Donglin Han, Lifeng Yan, Wufeng Chen, and Wan Li. Preparation of chitosan/graphene oxide composite film with enhanced mechanical strength in the wet state. Carbohydrate Polymers, 83(2):653–658, 2011.

[37] Oscar N Ruiz, K A Shiral Fernando, Baojiang Wang, Nicholas A Brown, Pengju George Luo, Nicholas D McNamara, Marlin Vangsness, Ya-Ping Sun, and Christopher E Bunker. Graphene oxide: a nonspecific enhancer of cellular growth. ACS nano, 5(10):8100–8107, 2011.

[38] François Perreault, Andreia Fonseca De Faria, Siamak Nejati, and Menachem Elimelech. Antimicrobial properties of graphene oxide nanosheets: why size matters. ACS nano, 9(7):7226–7236, 2015.

[39] I Barbolina, C R Woods, N Lozano, K Kostarelos, K S Novoselov, and I S Roberts. Purity of graphene oxide determines its antibacterial activity. 2D Materials, 3(2):25025, 2016.

[40] Karthikeyan Krishnamoorthy, Navaneethaiyer Umasuthan, Rajneesh Mohan, Jehee Lee, and Sang-Jae Kim. Antibacterial activity of graphene oxide nanosheets. Science of Advanced Materials, 4(11):1111–1117, 2012.

[41] Shaobin Liu, Ming Hu, Tingying Helen Zeng, Ran Wu, Rongrong Jiang, Jun Wei, Liang Wang, Jing Kong, and Yuan Chen. Lateral dimension-dependent antibacterial activity of graphene oxide sheets. Langmuir, 28(33):12364–12372, 2012.

[42] Achyut Konwar, Sanjeeb Kalita, Jibon Kotoky, and Devasish Chowdhury. Chitosan–Iron Oxide Coated Graphene Oxide Nanocomposite Hydrogel: A Robust and Soft Antimicrobial Biofilm. ACS applied materials & interfaces, 8(32):20625–20634, 2016.

[43] A Hebeish, Th I Shaheen, and Mehrez E El-Naggar. Solid state synthesis of starch-capped silver nanoparticles. International journal of biological macromolecules, 87:70–76, 2016.

[44] Xue-Fei Sun, Jing Qin, Peng-Fei Xia, Bei-Bei Guo, Chun-Miao Yang, Chao Song, and Shu-Guang Wang. Graphene oxide–silver nanoparticle membrane for biofouling control and water purification. Chemical Engineering Journal, 281:53–59, 2015.

[45] Leila Shahriary and Anjali A Athawale. Graphene oxide synthesized by using modified hummers approach. Int. J. Renew. Energy Environ. Eng, 2(01):58–63, 2014.

[46] Mohammad Mehrali, Emad Sadeghinezhad, Sara Tahan Latibari, Salim Newaz Kazi, Mehdi Mehrali, Mohd Nashrul Bin Mohd Zubir, and Hendrik Simon Cornelis Metselaar. Investigation of thermal conductivity and rheological properties of nanofluids containing graphene nanoplatelets. Nanoscale research letters, 9(1):15, 2014.

[47] Lei Huang, Hongtao Yang, Yanhua Zhang, and Wei Xiao. Study on synthesis and antibacterial properties of ag nps/go nanocomposites. Journal of Nanomaterials, 2016, 2016.

[48] Akihiro Ueda and Thomas K Wood. Connecting quorum sensing, c-di-gmp, pel polysaccharide, and biofilm formation in pseudomonas aeruginosa through tyrosine phosphatase tpba (pa3885). PLoS Pathog, 5(6):10–18, 2009.

[49] John D Brooks and Steve H Flint. Biofilms in the food industry: problems and potential solutions. International journal of food science & technology, 43(12):2163–2176, 2008.

[50] W Michael Dunne. Bacterial adhesion: seen any good biofilms lately? Clinical microbiology reviews, 15(2):155–166, 2002.

[51] George A O'toole and Roberto Kolter. Initiation of biofilm formation in pseudomonas fluorescens wcs365 proceeds via multiple, convergent signalling pathways: a genetic analysis. Molecular microbiology, 28(3):449–461, 1998.

[52] Nelson Durán, Priscyla D Marcato, Roseli De Conti, Oswaldo L Alves, Fabio Costa, and Marcelo Brocchi. Potential use of silver nanoparticles on pathogenic bacteria, their toxicity and possible mechanisms of action. Journal of the Brazilian Chemical Society, 21(6):949–959, 2010.